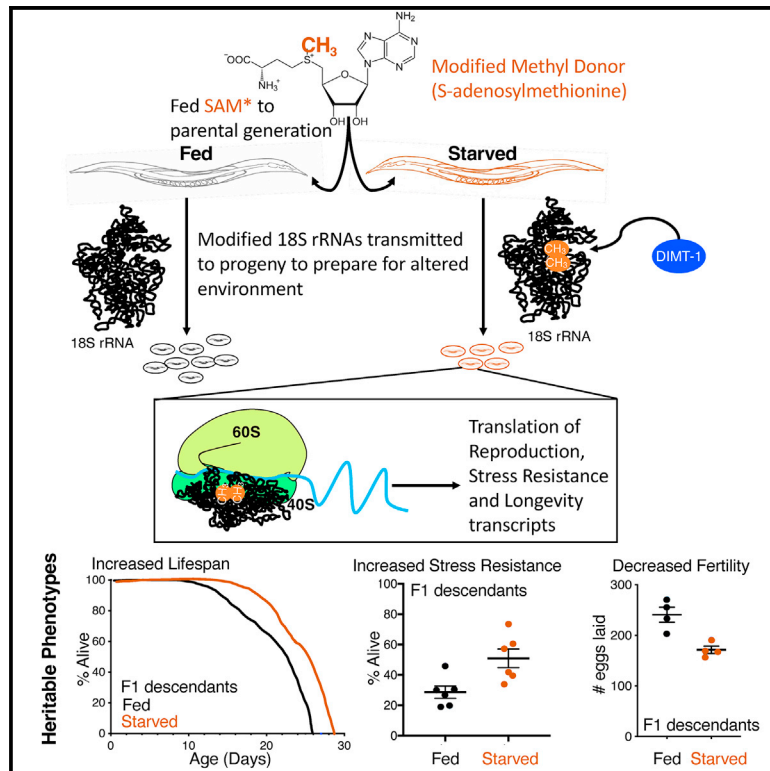**Article**

18S rRNA methyltransferases DIMT1 and BUD23 drive intergenerational hormesis

Graphical abstract

Authors

Noa Liberman, M. Hafiz Rothi,
Maxim V. Gerashchenko, ...,
Denis L.J. Lafontaine,
Vadim N. Gladyshev,
Eric Lieberman Greer

Correspondence

ericg@wustl.edu

In brief

Liberman et al. labeled and tracked heritable non-genetic information from parents to their children. They identified that $m^{6,2}A$ methylated rRNAs are transmitted across generations in response to parental starvation. This paper identified that ribosome heterogeneity helps subsequent generations prepare for harsh conditions.

Highlights

- Performed metabolic methyl-labeling to track heritable material across generations

- Identified heritable N6-dimethylation of adenosines 1735 and 1736 on ribosomal RNA

- Identified and characterized DIMT-1 and BUD-23 as $m^{6,2}A$ and m^7G methyltransferases

- Found *dimt-1* and *bud-23* necessary for transmission of heritable starvation response

CellPress

Molecular Cell

CellPress
OPEN ACCESS

Article

18S rRNA methyltransferases DIMT1 and BUD23 drive intergenerational hormesis

Noa Liberman,[1,2] M. Hafiz Rothi,[1,2] Maxim V. Gerashchenko,[3] Christiane Zorbas,[4] Konstantinos Boulias,[1,2] Fiona G. MacWhinnie,[2] Albert Kejun Ying,[1,2] Anya Flood Taylor,[2] Joseph Al Haddad,[2] Hiroki Shibuya,[1,2,7] Lara Roach,[1,2] Anna Dong,[2] Scarlett Dellacona,[2] Denis L.J. Lafontaine,[4] Vadim N. Gladyshev,[3] and Eric Lieberman Greer[1,2,5,6,8,*]

[1]Department of Pediatrics, HMS Initiative for RNA Medicine, Harvard Medical School, Boston, MA, USA
[2]Division of Newborn Medicine, Boston Children's Hospital, Boston, MA, USA
[3]Division of Genetics, Department of Medicine, Brigham & Women's Hospital, Harvard Medical School, Boston, MA 02115, USA
[4]RNA Molecular Biology, Fonds de la Recherche Scientifique (F.R.S./FNRS), Université libre de Bruxelles (ULB), Biopark Campus, 6041 Gosselies, Belgium
[5]Department of Pediatrics, Washington University School of Medicine, St. Louis, MO 63110, USA
[6]Department of Genetics, Washington University School of Medicine, St. Louis, MO 63110, USA
[7]Present address: RIKEN Center for Biosystems Dynamics Research, Kobe, Japan
[8]Lead contact
*Correspondence: ericg@wustl.edu
https://doi.org/10.1016/j.molcel.2023.08.014

SUMMARY

Heritable non-genetic information can regulate a variety of complex phenotypes. However, what specific non-genetic cues are transmitted from parents to their descendants are poorly understood. Here, we perform metabolic methyl-labeling experiments to track the heritable transmission of methylation from ancestors to their descendants in the nematode *Caenorhabditis elegans* (*C. elegans*). We find heritable methylation in DNA, RNA, proteins, and lipids. We find that parental starvation elicits reduced fertility, increased heat stress resistance, and extended longevity in fed, naïve progeny. This intergenerational hormesis is accompanied by a heritable increase in N6'-dimethyl adenosine ($m^{6,2}A$) on the 18S ribosomal RNA at adenosines 1735 and 1736. We identified DIMT-1/DIMT1 as the $m^{6,2}A$ and BUD-23/BUD23 as the m^7G methyltransferases in *C. elegans* that are both required for intergenerational hormesis, while other rRNA methyltransferases are dispensable. This study labels and tracks heritable non-genetic material across generations and demonstrates the importance of rRNA methylation for regulating epigenetic inheritance.

INTRODUCTION

Organisms adapt to different environmental cues and activate stress response pathways to survive under adverse conditions. The ability of an organism to address these conditions not only relies on its genetic information but also on the integration of non-genetic (epigenetic) information. This non-genetic inheritance allows organisms to adapt to extreme environmental conditions and transmit this information to their progeny without genetic mutations. By circumventing mutations, stressed organisms can return to basal conditions once the environment reverts to a more favorable state. Although the inheritance of genetic information is well established, inheritance of epigenetic information has been a matter of debate. Even so, growing evidence, both phenotypic and molecular, has greatly supported the biological existence of this concept. Epigenetic inheritance has been shown to regulate physical appearance, energy metabolism, behavioral state, and longevity in species ranging from yeast to humans.[1–4] More specifically, epigenetic inheritance

has been linked to inter- and transgenerational mechanisms that regulate the response to various environmental cues and stresses[1–3] including heat stress[5–10] and starvation.[11–17] Food availability is one of the most robust and reproducible environmental cues to induce epigenetic inheritance across a wide variety of species.[1,2,4] Correlative evidence suggests that when humans experience famine *in utero*, such as in the Dutch Hunger study or the great Chinese famine,[18–22] obesity, diabetes, and cardiovascular diseases can arise later in life. However, what specific non-genetic information is passed from parents to their children to warn the next generation of reduced food availability is still unknown. Studies over the past decade have identified epigenetic phenomena and characterized DNA methylation, histone-modifying enzymes, small RNA pathways, and prions as necessary components for epigenetic inheritance.[1–4] Although many groups have identified critical epigenetic regulators as being required for epigenetic inheritance, here we aimed to directly demonstrate what specific epigenetic information is transmitted from parents to their progeny.
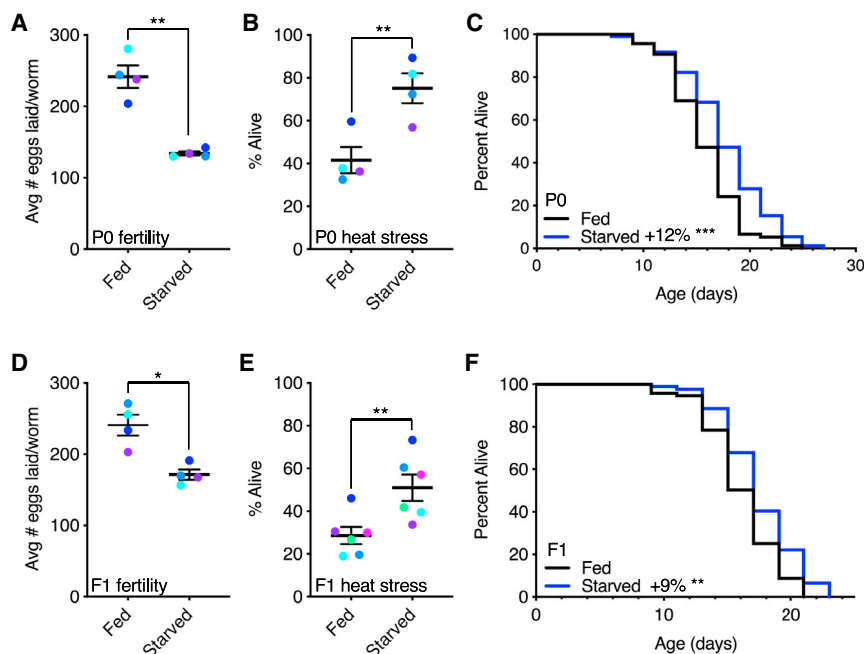
Figure 1. Parental starvation causes intergenerational hormesis in descendants

(A) Starvation causes a reduction in reproduction. Each column represents the mean ± SEM of 4 independent experiments performed in three plates with 10 worms per plate. Dots are color coded to display matched independent experiments.

(B) Starvation causes an increase in survival in response to 37°C heat stress for 6 h. Each column represents the mean ± SEM of 4 independent experiments performed in 3 plates with 30 worms per plate.

(C) Starvation causes an increase in longevity. Each condition represents three plates of ~30 worms per plate. This is a representative experiment that has been performed 5 times (Table S1).

(D) Naïve F1 progeny whose parents were starved have reduced fertility relative to progeny whose parents were fed. Each column represents the mean ± SEM of 4 independent experiments performed in 3 plates with 10 worms per plate.

(E) Naïve F1 progeny whose parents were starved display an increase in survival in response to 37°C heat stress for 6 h. Each column represents the mean ± SEM of 6 independent experiments performed in 3 plates with 30 worms per plate.

(F) Naïve F1 progeny whose parents were starved have an increase in longevity. Each condition represents three plates of ~30 worms per plate. This is a representative experiment that has been performed 5 times (Table S1). * $p < 0.05$ and ** $p < 0.01$ as assessed by paired t test. ** $p < 0.01$ and *** $p < 0.001$ as assessed by log-rank (Mantel-Cox) test. See also Figure S1 and Table S1.

RESULTS

Parental starvation induces intergenerational hormesis in progeny

We first established a system where environmental manipulations caused robust reproducible generational transmission of phenotypes. Parental starvation has been shown to cause altered levels of small RNAs,[11–13] reduce fertility,[14] and increase lifespan, size, and heat stress resistance[11,15,16] in descendants for one or several generations in *Caenorhabditis elegans* (*C. elegans*). Consistent with previous work,[11,15,16] we found that 7 days of starvation at the first larval stage (L1) of *C. elegans* development, caused a reduction in fertility, an increase in heat stress resistance, and a subtle extension in lifespan (Figures 1A–1C). Furthermore, parental (P0) starvation caused naïve F1 descendants to also display increased heat stress resistance, reduced fertility, and a subtle extension in lifespan (Figures 1D–1F). These phenotypes persisted in the F2 generation but reverted back to the levels seen in descendants of well-fed worms by the F3 generation (Figures S1A–S1D). Parental starvation at the L1 stage for 3 days was sufficient to induce decreased fertility and increased heat stress resistance in the exposed generation but not in naïve F1 descendants (Figures S1E–S1H). Thus, parental starvation induced an adaptive response not only in the generation that was exposed to the environmental stress but also in their naïve descendants providing the exposure to stress was sufficiently prolonged. The observation that these phenotypes do not persist after the F2 generation suggests that these phenotypes are regulated by reversible epigenetic information.

Heritable methylation is elevated in the RNA of descendants of starved parents

To determine what specific epigenetic information is passed from parents to their progeny, we first designed and optimized a system for tracking inherited non-genetic material. We decided to focus on methylation, due to the diversity of substrates and the use of this chemical moiety to reversibly alter their function and to respond to the environment. S-Adenosylmethionine (SAM) is the predominant methyl donor for DNA, RNA, proteins, and lipids.[23] We therefore used modified SAM where the hydrogens of the methyl group are replaced with the heavy isotope deuterium (D) or the radioactive isotope tritium (^{3}H) to allow us to detect and track methylation. Modified SAM and methionine have been used to detect direct methylation targets of RNA methyltransferases and histone methyltransferases.[24–30] To ensure that modified SAM could be used efficiently by methyltransferases, we performed control *in vitro* methylation assays with SAM-D$_3$ and SAM-^{3}H$_3$ and found that both were efficiently utilized (Figure S2).

To determine whether methylation is transmitted from parents to progeny and to examine which substrates were heritably methylated, we administered SAM-^{3}H$_3$ to wild-type (WT) early larval stage 4 (L4) *C. elegans* and then tested for the incorporation of ^{3}H in the total lysate as well as purified DNA, RNA, and lipids of adult worms and their progeny. Since the modified methyl label is fed only in the parental generation, any detected ^{3}H in the descendant generation must represent heritable methylation. Indeed, we found that we could detect methylated DNA, RNA, proteins, and lipids in the P0 worms and in naïve F1 eggs (Figure 2A). We were therefore able to track epigenetic

material from ancestors to their descendants. Since each worm has ~250 progeny, and each progeny develops from a single cell into 959 somatic and ~2,000 germ cells, it is not feasible, at this stage because of detection sensitivity limitations, to track heritable methylation to the F2 generation. Since SAM is relatively unstable[31,32] it is most likely that any ^{3}H detected in the progeny would have been incorporated into heritably methylated material in the parents and transmitted to the progeny rather than taken up by or transmitted in the form of SAM-^{3}H$_3$ to the progeny themselves.

The growing evidence for RNA's role in transgenerational inheritance led us to initially focus our study on heritable RNA methylation. It will be interesting to look at other heritably methylated substrates in subsequent studies as there is likely a reinforcing network of multiple heritable molecules that can regulate transgenerational epigenetic inheritance. We next wanted to determine whether starvation would affect the amount of heritable RNA methylation. We kept arrested L1 worms in the absence of food for 7 days, followed by recovery of the worms on food until they reached the L4 stage. At this point, we supplemented the worms with SAM-^{3}H$_3$ and let them continue developing to become egg-bearing adults. F1 eggs were extracted, RNA purified, and incorporation of radioactivity was measured by scintillation counting (Figure 2B). We found an increase in detection of radioactivity in RNA of starved parents and their naive progeny (Figure S2C). Similarly, we found an increase in radioactive methyl groups in P0 and F1 generations when ^{3}H-methionine was fed to the starved P0 at the L4 stage (Figure 2C). Importantly, starved worms did not consume more food once they reached the L4 stage, after recovery on food (Figure S2D), suggesting that there is not an increase in consumption of the methyl donor. Furthermore, we did not detect an increase in heritable methylation in response to parental heat stress (Figures S2E and S2F), an environmental cue that has also been shown to elicit transgenerational effects in *C. elegans*,[6,7] indicating that this increase in heritable RNA methylation is a specific response to parental starvation.

Heritable dimethylation at the N6 position of adenines is elevated on the 18S ribosomal RNA of descendants of starved parents

To examine in an independent manner whether and where methylation increased in RNA of descendants whose parents were starved, we repeated the starvation assay feeding methionine-D$_3$ to the parents (Figure 2B). Since ribosomal RNA (rRNA) constitutes >80% of the total RNA in a cell,[33] we first looked for changes in heritable methylation on rRNA. To determine which rRNAs displayed increased heritable methylation, we isolated total RNA from F1 eggs, whose parents were either fed or starved and were supplemented with methionine-D$_3$. rRNA populations 26S, 18S, and 5.8/5S were gel isolated and run through ultra-high-performance liquid chromatography coupled with triple-quadrupole tandem mass spectrometry (UHPLC-MS/MS) on each population of rRNA. We found a consistent increase in dimethylated N6 adenosine (m^{6,2}A) on the 18S rRNA in response to parental starvation (Figure 2D). We did not observe a consistent increase in methylation of other residues on the 18S or 26S rRNA (Figure 2D), suggesting that there is not a general increase

in rRNA methylation but a specific increase in 18S m^{6,2}A. Together, this data suggests that starvation causes parents to transmit increased m^{6,2}A methylated 18S rRNA to their naïve descendants.

Knockdown of *dimt-1* decreases 18S rRNA N6-dimethyladenosine, and deletion of *bud-23* decreases 18S rRNA N7-methylguanosine

To determine whether m^{6,2}A is important for the intergenerational hormesis phenotypes we observed (Figure 1), we first sought to identify the 18S rRNA N6-dimethyltransferase. The 18S is N6-dimethylated at two adjacent adenosines, 1850 and 1851, in mammals,[34] which correspond to adenosine 1735 and 1736 in *C. elegans*. These adjacent adenosines are located at the decoding site of the small ribosomal subunit, where the mRNA is "read," display conserved methylation from bacteria to humans, and have been shown to be methylated by dimethyladenosine transferase 1 (DIMT1) in yeast and humans.[35–38] Another nucleoside on the *Homo sapiens* (*H. sapiens*) 18S rRNA, also in the vicinity of the mRNA channel, has been shown to be methylated in yeast and humans[34]—this is guanosine 1639, which corresponds to guanosine 1531 in *C. elegans*. The putative N7-guanosine methyltransferase Bud23 in yeast and WBSCR22 in humans has been proposed to methylate this guanosine.[38–40] Both DIMT1 and Bud23 are important for rRNA processing.[38,41] These enzymes have clear *C. elegans* homologs, and E02H1.1 shows homology to DIMT1, which we renamed *dimt-1*, while C27F2.4 shows homology to Bud23/WBSCR22,[42] which we renamed *bud-23*. To test whether DIMT-1 and BUD-23 were m^{6,2}A and m^{7}G 18S rRNA methyltransferases, we knocked down *dimt-1* and *bud-23* by feeding WT worms bacteria expressing an empty vector (EV) or double-stranded RNA against each of these genes. We next isolated 26S, 18S, and 5.8S/5S rRNAs and performed UHPLC-MS/MS on each population of rRNA. We found no discernable changes in mRNA methylation (Figure S3A) or rRNA methylation on the 26S or 5.8S/5S rRNAs in response to *dimt-1* or *bud-23* knockdown. However, we did detect a significant decrease in m^{6,2}A 18S rRNA levels without changes in other methylated bases in response to *dimt-1* knockdown (Figures 3A and S3B). Additionally, knocking down *bud-23* caused a significant decrease specifically in 18S rRNA m^{6,2}A and m^{7}G (Figures 3A and S3B). To ascertain whether the change in 18S rRNA methylation was due to *bud-23* knockdown rather than an off-target effect of the small interfering RNA, we examined RNA methylation in a genetic mutant strain *bud-23(tm5768)* which contains a large deletion of the putative methyltransferase domain.[42] This mutant strain displayed a complete elimination of m^{7}G, a substantial decrease in m^{6,2}A, and, interestingly, a near doubling of m^{6}A without changing other methylations on the 18S rRNA (Figures 3B and S3C). To determine whether the change in m^{7}G was due to BUD-23 activity, we generated transgenic rescue strains of WT or G63E/D82K double-mutant *bud-23* driven by the ubiquitous *eft-3* promoter in a *bud-23(tm5768)* mutant background (P$_{eft-3}$::*bud-23* WT and P$_{eft-3}$::*bud-23* G63E/D82K). Equivalent amino acids substitutions have been shown to eliminate WBSCR22 activity in HEK293 cells.[38,40] Six independent
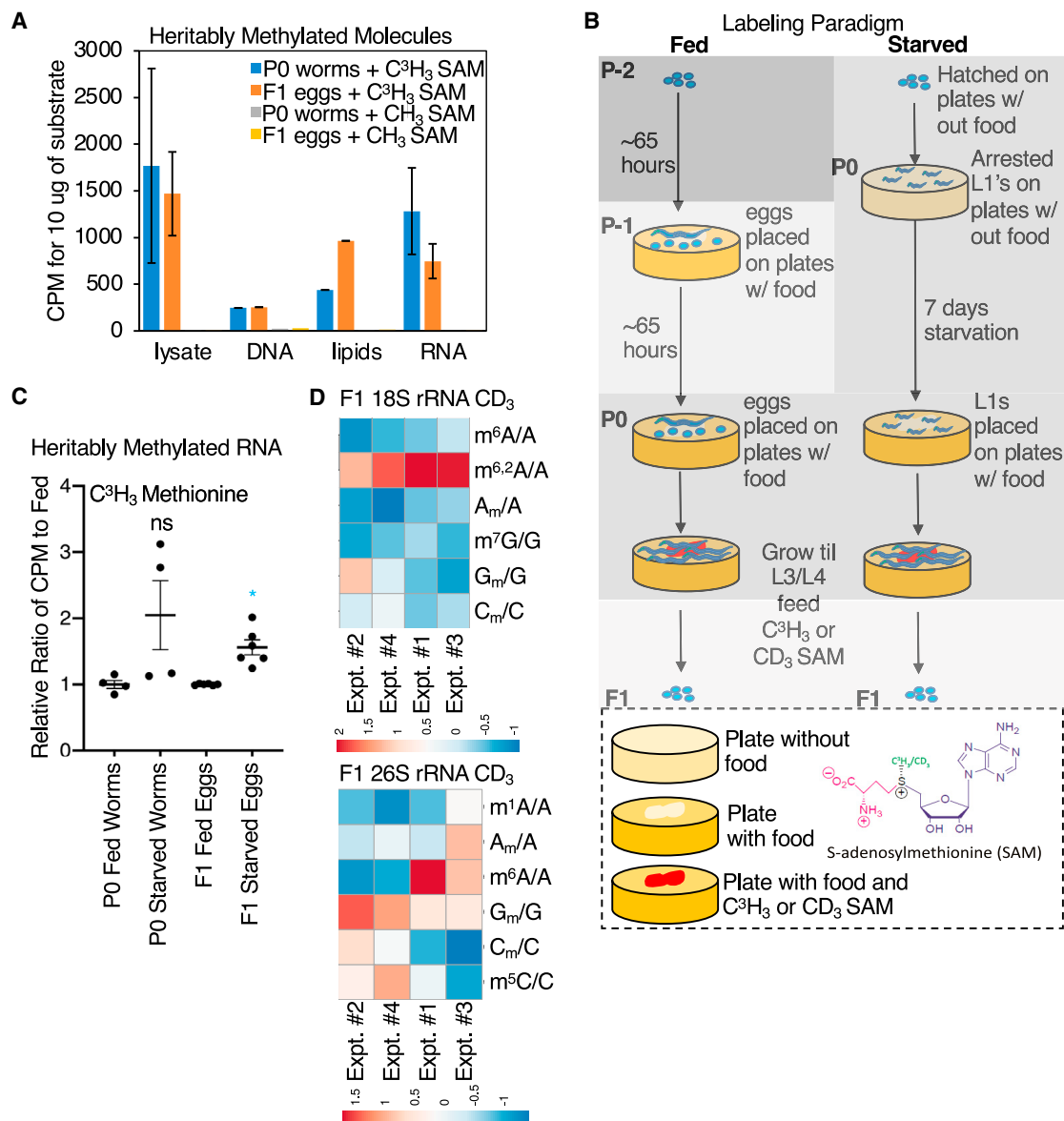
Figure 2. Descendants of starved parents display increased m^{6,2}A 18S rRNA methylation

(A) Radioactive methyl groups were detected in the total lysate, DNA, lipids, or RNA of P0 worms fed SAM-C^{3}H$_3$ (blue bars) and their F1 progeny (orange bars) as detected by scintillation counting. No radioactive signal was detected in worms (gray bars) or their progeny (yellow bars) fed non-radioactive SAM. Each bar represents 5–6 experiments for total lysate, 1 experiment for DNA, 1 experiment for lipids, and 8–9 experiments for RNA. Each sample was normalized to the amount of material in that sample.

(B) Scheme for feeding paradigm to administer tritiated or deuterated SAM to fed or starved P0 L4 worms.

(C) Increased radioactive signal is detected in the RNA of both the P0 worms as well as their naïve F1 progeny when the P0 generation is starved relative to fed when fed methionine-C^{3}H$_3$. Each column represents the mean ± SEM of 4 or 6 independent experiments. ns, not significant, * p < 0.05 as assessed by one-way ANOVA and Tukey's multiple comparisons test.

(D) Naïve F1 progeny whose parents were starved display elevated m^{6,2}A/A levels on the 18S rRNA relative to F1 progeny whose parents were fed as detected by UHPLC-ms/ms. P0 parents were fed methionine-CD$_3$, and RNA was extracted from F1 eggs. This heatmap represents the relative fold change for 4 independent experiments, where each experiment is displayed in one column.

See also Figure S2.

P_{eft-3}::bud-23 WT but not six independent P_{eft-3}::bud-23 G63E/D82K lines rescued the 18S rRNA m^{7}G as well as the m^{6,2}A levels (Figure 3C), indicating that BUD-23 catalytic activity is required for 18S rRNA methylation. Together, these results suggest that DIMT-1 regulates 18S rRNA m^{6,2}A while BUD-23 regulates both 18S rRNA m^{7}G and m^{6,2}A, indicating that in *C. elegans*, the two proteins interact functionally on 40S precursor subunits.
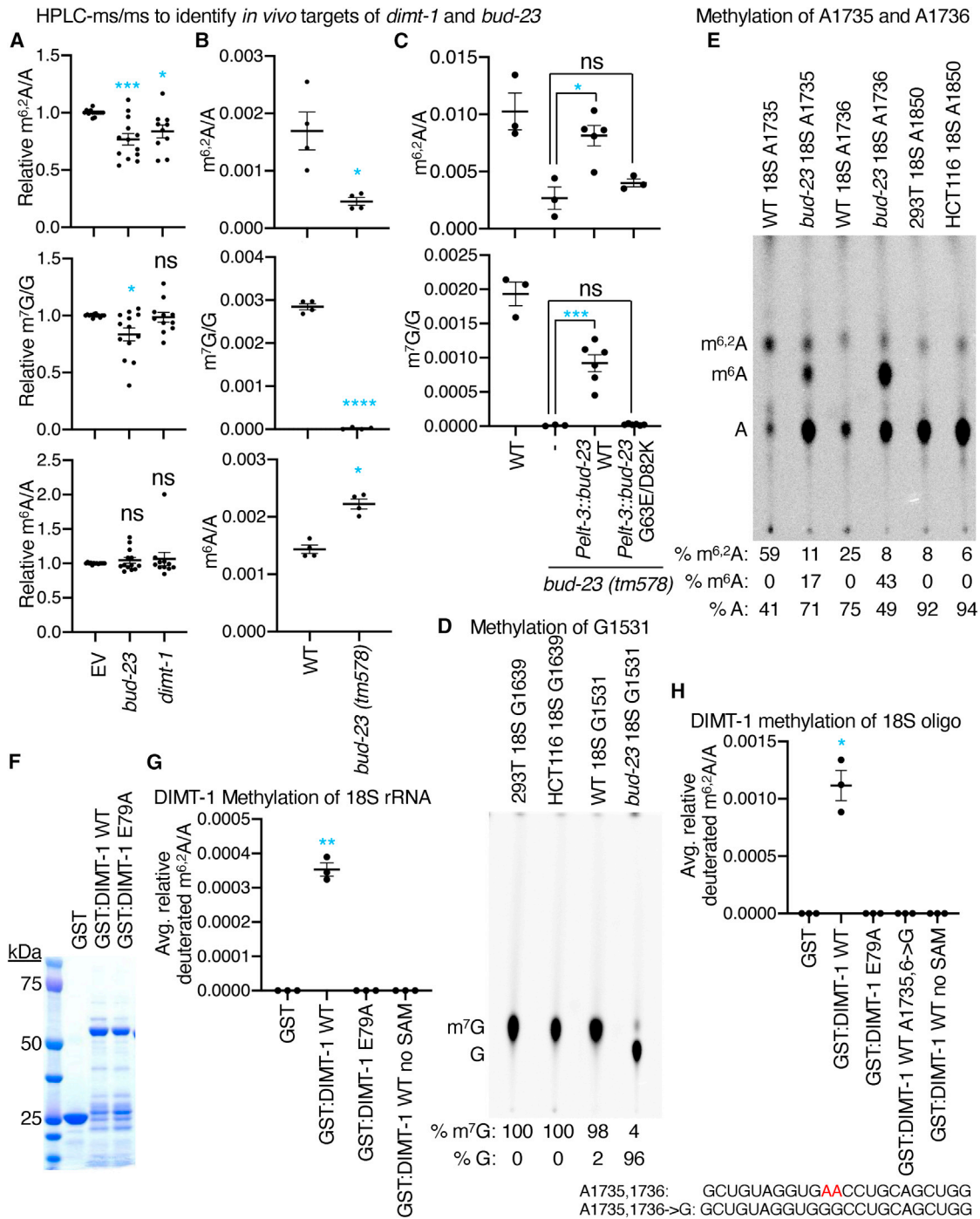
Figure 3. DIMT-1 and BUD-23 are m^{6,2}A and putative m^7G 18S rRNA methyltransferases

(A) Knockdown of *dimt-1* and *bud-23* causes a decrease in m^{6,2}A and m^{6,2}A and m^7G levels on 18S rRNA, respectively, relative to empty vector (EV) control knockdown as assessed by UHPLC-MS/MS. There was no significant effect on m^6A levels or other methylation marks on the 18S rRNA (Figure S3B). Each bar represents the mean ± SEM of 12 independent replicates. ns, not significant, * $p < 0.05$, *** $p < 0.001$ as assessed by one-way ANOVA and Holm-Sidak's multiple comparisons test.

(B) *bud-23(tm5768)* mutant strain displays a decrease in m^7G and m^{6,2}A levels while showing increased m^6A levels on the 18S rRNA as assessed by UHPLC-MS/MS. There was no significant effect on other methylation marks on the 18S rRNA (Figure S3C). Each bar represents the mean ± SEM of 4 independent experiments. * $p < 0.05$, **** $p < 0.0001$ as assessed by paired t test.

(legend continued on next page)

Interestingly, the decrease in $m^{6,2}A$ was accompanied by an increase in 18S rRNA m^6A in response to deletion of *bud-23*. Previously, we demonstrated that there is a single adenine on the *C. elegans* 18S rRNA that is constitutively methylated by *metl-5*/METTL5.[30] Therefore, this finding raises the possibility that m^7G methylation is a necessary precursor for $m^{6,2}A$ methylation, and without m^7G methylation, the adenines that would normally be dimethylated to produce $m^{6,2}A$ are instead singly methylated to produce m^6A. We could not examine *dimt-1* mutant strains as this gene is essential for viability.

To determine whether A1735 and A1736 on the 18S rRNA are the $m^{6,2}A$ methylated nucleosides, we performed primer extension assays. We found the primers were extended until A1735 (Figure S3D), suggesting that the conserved residue adenosine 1735 is modified in *C. elegans* as it is in humans and yeast. To independently confirm whether A1735, A1736, and G1531 are the methylated nucleosides, we performed site-specific cleavage and radioactive labeling followed by ligation-assisted extraction and thin-layer chromatography (SCARLET)[43] on 18S rRNA purified from WT and *bud-23(tm5768)* mutant worms. We identified that G1531 is N7-methylated constitutively in WT *C. elegans* (Figure 3D). The *bud-23(tm5768)* mutant worms 18S rRNA were almost completely unmethylated at G1531 (Figure 3D), suggesting that BUD-23 is responsible for N7-methylation of this specific guanosine. We further found that A1735 and A1736 were $m^{6,2}A$ methylated (Figure 3E). Interestingly in the *bud-23(tm5768)* mutant worms, A1735 and A1736 displayed reduced dimethylation and increased monomethylation on the N6 position (Figure 3E). Because $m^{6,2}A$ interferes with Watson-Crick base pairing, the SCARLET method cannot accurately quantify the percentage methylation that is occurring at these residues.[43] However, we can conclude that A1735 and A1736, as well as the human 18S A1850, are not constitutively $m^{6,2}A$, and therefore, these residues are poised to respond to environmental conditions. Interestingly, a recent report also found that in *Saccharomyces cerevisiae* and mammalian cell lines, these two residues can be N6-monomethylated ~4% of the time and that m^6A increases 3- to 8-fold higher in response to sulfur starvation, deprivation of methionine or SAM decreases.[44] Thus, our results

validate that the conserved nucleosides are $m^{6,2}A$ and m^7G methylated in *C. elegans*, and *bud-23* deletion limits $m^{6,2}A$ and facilitates m^6A of these precise adenosines.

DIMT-1 dimethylates 18S rRNA on the N6 position of adenosines 1735 and 1736

To determine whether DIMT-1 directly methylates 18S rRNA, we expressed a glutathione S-transferase (GST)-tagged *dimt-1* in bacteria, purified DIMT-1 (Figure 3F), and analyzed its ability to methylate 18S rRNA. DIMT-1 specifically increased $m^{6,2}A$ on 18S rRNA *in vitro* (Figure 3G). To further verify that DIMT-1 is an 18S rRNA methylase, we mutated the conserved glutamic acid E79, as the equivalent amino acid is essential for human DIMT-1's catalytic activity.[37] Mutation of E79 to alanine (E79A) ablated the N6-adenosine dimethyltransferase activity on 18S rRNA (Figure 3G). To determine whether DIMT-1 could methylate A1735 and A1736, we performed *in vitro* methylation assays with recombinant DIMT-1 using 23-nucleotide synthetic oligonucleosides consisting of A1735 and A1736 and flanking nucleosides from the 18S rRNA sequence (Figure 3H). We found that WT DIMT-1, but not catalytically dead DIMT-1, methylated this oligonucleoside (Figure 3H). This methylation was specific to A1735 and A1736, as no methylation was detected in *in vitro* methylation assays using the same oligos where adenosines 1735 and 1736 had been replaced by guanosines (Figure 3H). Together these results show that DIMT-1 is the direct 18S rRNA $m^{6,2}A$ methyltransferase both *in vitro* and *in vivo*.

Ribosome profiling reveals that parental starvation or *bud-23* or *dimt-1* knockdown alters translation of genes involved in longevity and the stress response

rRNA methylation alters the association of the ribosome to particular transcripts.[30,45,46] DIMT1 binding to pre-rRNA is important for rRNA processing,[38,41] presumably that is the reason why *dimt-1* deletion mutants are not viable. We wanted to determine whether the changes in ribosome occupancy were due to changes in rRNA processing or in binding of the ribosome to specialized transcripts. To determine whether knockdown of *dimt-1*, which caused a ~70% decrease in *dimt-1* mRNA (Table S2) and a ~30% decrease

---

(C) *bud-23* WT but not the catalytically inactive mutant G63E/D8K overexpression lines in *bud-23(tm5768)* mutant worms rescues 18S rRNA m^7G and $m^{6,2}A$ methylation levels, as assessed by UHPLC-MS/MS. Each bar represents the mean ± SEM of 3–6 independent rescue strains. ns, not significant, * $p < 0.05$, *** $p < 0.001$ as assessed by one-way ANOVA and Tukey's multiple comparisons test.

(D) SCARLET reveals that G1531 in *C. elegans* 18S rRNA is N7-methylated, and this methylation is reduced in *bud-23(tm5768)* mutant worms. Quantification of signal intensities below. Control oligos were run for reference as to where guanosine and m^7G should run but are not shown. 18S rRNA methylation at G1639 in human cell lines is used as a positive control.

(E) SCARLET reveals that A1735 and A1736 in *C. elegans* 18S rRNA are N6-dimethylated, and this methylation is reduced in *bud-23(tm5768)* mutant worms and replaced with N6-monomethylation. Control oligos of where adenosine and m^6A were run but are not shown in this blot. 18S rRNA methylation at A1850 in human cell lines is used as a positive control. The calculation below depicts relative intensity of each residue but is not quantitative due to the effects that $m^{6,2}A$ has on Watson-crick base pairing.

(F) Coomassie staining of SDS-PAGE gel reveals that GST-tagged DIMT-1 WT and E79A mutant proteins migrate at the same location.

(G) WT GST-tagged DIMT-1 but not the catalytically inactive mutant E79A is able to methylate 18S rRNA purified from *bud-23* mutant worms, as assessed by UHPLC-MS/MS when deuterated S-adenosyl methionine was used as the methyl donor. 18S rRNA has 451 adenosines so this calculates the increase in $m^{6,2}A$ on all 451 adenosines despite increasing on 2 specific adenosines. Each column represents the mean ± SEM of three independent experiments. ** $p < 0.01$ as assessed by paired t test.

(H) WT but not E79A mutant GST-tagged DIMT-1 methylates an oligo containing the sequence surrounding 18S A1735 and A1736. When A1735 and A1736 are replaced with guanosines, no methylation is detected despite the presence of additional adenosines in the oligo. There are 4 or 2 adenosines present in oligos, so analysis examines the increase in $m^{6,2}A$ on all adenosines even though it is only increasing on 2 specific adenosines. (Top) The oligo sequence is displayed with A1735 and A1736 highlighted in red (bottom) each column represents the mean ± SEM of three independent experiments. * $p < 0.05$ as assessed by paired t test. See also Figure S3.

in 18S rRNA m^{6,2}A (Figure 3A), was sufficient to alter rRNA processing, we measured rRNA intermediates after *dimt-1* knockdown. We first measured levels of 18S and 26S rRNA by real-time RT-PCR and found that neither parental starvation nor knockdown of either rRNA methyltransferase caused a significant change in levels of rRNA (Figure S4A). This was further confirmed by ethidium bromide staining of extracted RNAs (Figure S4B). We found that knockdown of *dimt-1* in *C. elegans* caused a very subtle slowing of 18S maturation (Figures S4C–S4F), suggesting that the effects on ribosome occupancy are primarily through means independent of rRNA processing.
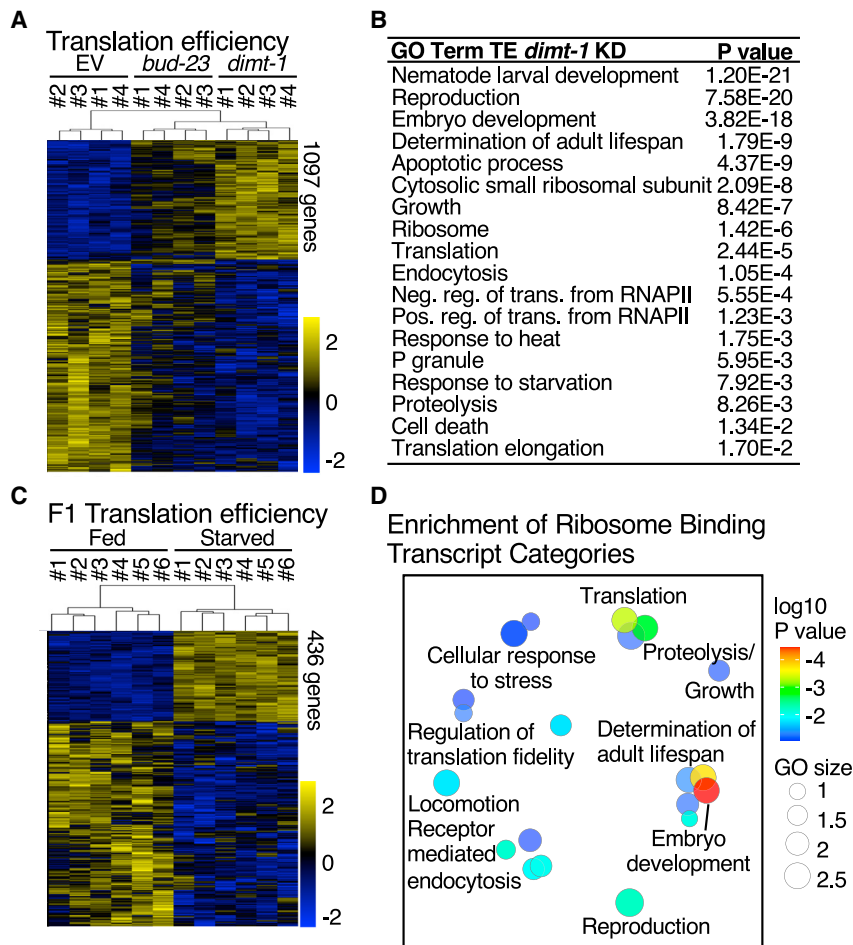
To determine the consequence of starvation-induced heritable rRNA methylation on translation, we first examined the polysome profile and found no change in polysome profiles in descendants whose parents had been fed or starved (Figures S4G and S4H). Thus, parental starvation does not globally affect polysome profiles in their descendants. To determine whether parental starvation alters ribosome binding to specific transcripts, ribosome-bound RNAs and total cellular polyadenylated-selected RNA were sequenced[47] in six independent biological replicates from F1 eggs of WT fed or starved parents and four independent biological replicates from eggs of EV control or *bud-23* and *dimt-1* knockdown worms. We first analyzed the transcription changes in response to *bud-23* and *dimt-1* knockdown. Transcriptional changes would not be direct consequences of manipulating the rRNA methylation; however, changes in translation will lead to changes in transcription.[48,49] We found a high degree of overlap between misregulated genes after *bud-23* and *dimt-1* knockdown (Figures S5A–S5C; Table S2, 1,224 of the 1,319 upregulated and 731 of the 882 downregulated genes p = 0 by hypergeometric probability). A gene ontology (GO) analysis of the shared misregulated genes in response to *bud-23* and *dimt-1* knockdown revealed genes involved in reproduction, translation, longevity, and growth (Figure S5D). Parental starvation also caused a change of gene expression enriched in the response to heat, translation, and the unfolded protein response (Figures S5E and S5F; Table S2). Parental starvation had no effect on the expression levels of *bud-23* or *dimt-1* themselves (Figure S5G). Despite the fact that EV, *bud-23*, and *dimt-1* knockdown worms were fed HT115(DE3) bacteria and the F1 WT fed and F1 WT starved were fed OP50-1 bacteria, there was still a significant overlap between downregulated genes upon knockdown of *bud-23* and *dimt-1* and upregulated genes in response to parental starvation (Figures S5H, 195 of the 731 p < 7E−27 by hypergeometric probability). Interestingly, the shared pathways which become transcriptionally dysregulated in response to knockdown of the methyltransferases and parental starvation include translation, the response to heat, development, and reproduction (Figure S5I), mirroring some of the phenotypes observed in response to parental starvation (Figure 1). Examining the shared transcriptionally dysregulated pathways in an alternative annotation methodology, WormCat,[50] also revealed dysregulation of genes involved in stress responses and the ribosome (Figure S5J). This suggests that a portion of these intergenerational phenotypes might be due to transcriptional dysregulation, as a likely indirect consequence of translation rewiring caused by transmission of differentially modified ribosomes (see below).

To determine if parental starvation and *bud-23* and *dimt-1* knockdown also altered the ribosome binding to specific transcripts, we sequenced ribosome-bound RNAs from the same six and four biological replicates and normalized that to transcript levels to measure translation efficiency. We observed a high degree of reproducibility within our replicate samples (Figure S5K; Table S3). Similarly, to the shared transcriptional response to knockdown of *bud-23* and *dimt-1*, there was also a similar translational response as assessed by translation efficiency (Figures 4A and S5L). We found that 1,103 transcripts were differentially bound after *dimt-1* knockdown and 62 transcripts were differentially bound after *bud-23* knockdown. Although we only detected 62 differentially bound transcripts after *bud-23* knockdown that met our rigorous statistical standards, 52 of these genes were also differentially bound by the ribosome after *dimt-1* knockdown (p < 1.6E−46 by hypergeometric probability). GO analysis of shared differentially bound transcripts after *dimt-1* and *bud-23* knockdown revealed pathways involved in determination of adult lifespan, development, and reproduction (Figures 4B, S5M, and S5N). Parental starvation also caused different translation efficiency (Figures 4C and S5O). Interestingly, there was a high degree of overlap between differentially translated genes in response to parental starvation and *dimt-1* knockdown (Figure S5P, 76 of 443, p < 1E−9 by hypergeometric probability), which included transcripts involved in the altered phenotypes observed after parental starvation, including longevity, reproduction, and stress response (Figures 4D and S5Q). Together, these results suggest that parental starvation, through 18S rRNA methylation by the m^{6,2}A and m^{7}G methyltransferases, causes both transcriptional and translational changes that could be responsible for the observed intergenerational phenotypic changes. This raises the possibility that parental starvation can transmit specifically modified rRNAs to their naïve descendants to prime the descendant worms for possible starvation.

DIMT-1 and BUD-23 are required for intergenerational hormesis in response to starvation

To determine whether the m^{6,2}A modification is important for the observed intergenerational hormesis phenotypes (Figure 1), we examined whether knockdown of *bud-23* or *dimt-1* would eliminate these phenotypes. Knockdown of *dimt-1* eliminated the heritable increase in m^{6,2}A (Figure S6A). Knockdown of *bud-23* or *dimt-1* had no effect in the parental generation response to starvation since starvation of P0 *bud-23* or *dimt-1* knockdown worms reduced fertility and increased heat stress resistance (Figures 5A and 5B). Excitingly, however, knockdown of either *bud-23* or *dimt-1* eliminated the increased heat stress resistance and reduction in fertility in the naïve F1 generation progeny whose parents had been starved relative to those whose parents had been fed (Figures 5C and 5D). Knockdown of *bud-23* or *dimt-1* did cause a reduction in fertility and increase in heat stress resistance in the fed progeny relative to fed control progeny, suggesting that, independent of parental starvation, 18S rRNA m^{6,2}A and m^{7}G methylation is important for fertility and stress resistance. Despite the starvation-independent consequence of *bud-23* or *dimt-1* knockdown in F1 generation progeny, there was still the possibility of a further reduction in fertility

A

Translation efficiency

B

GO Term TE *dimt-1* KD	P value
Nematode larval development	1.20E-21
Reproduction	7.58E-20
Embryo development	3.82E-18
Determination of adult lifespan	1.79E-9
Apoptotic process	4.37E-9
Cytosolic small ribosomal subunit	2.09E-8
Growth	8.42E-7
Ribosome	1.42E-6
Translation	2.44E-5
Endocytosis	1.05E-4
Neg. reg. of trans. from RNAPII	5.55E-4
Pos. reg. of trans. from RNAPII	1.23E-3
Response to heat	1.75E-3
P granule	5.95E-3
Response to starvation	7.92E-3
Proteolysis	8.26E-3
Cell death	1.34E-2
Translation elongation	1.70E-2

C

F1 Translation efficiency

D

Enrichment of Ribosome Binding Transcript Categories

Figure 4. Altered translation of genes involved in development, translation, longevity, and stress response in response to *bud-23* and *dimt-1* knockdown and parental starvation

(A) High degree of overlap between differentially ribosome-bound transcripts after *bud-23* or *dimt-1* knockdown revealed by heatmap. Each column represents an independent biological replicate.

(B) GO analysis of transcripts that are differentially bound after knockdown of *dimt-1* reveals the importance of 18S $m^{6,2}A$ methylation in regulation of development, reproduction, longevity, and response to heat.

(C) Heatmaps of the 436 differentially ribosome-bound transcripts after parental starvation. Each of 6 independent biological replicates cluster together.

(D) Revigo plots reveal relative enrichment of coordinately dysregulated ribosome binding to transcripts involved in response to stress, reproduction, and lifespan regulation in response to parental starvation and *dimt-1* knockdown. Proximity of bubbles reflects the similarity of terms, color intensity represents p value of enrichment, and size of the bubbles reflects how many genes are in the gene set depicted.

See also Figures S4 and S5 and Tables S2 and S3.

or increase in heat stress resistance, which did not occur, suggesting that BUD-23 and DIMT-1 are necessary for the transmission of intergenerational hormesis. Note that *C. elegans* consume the *E. coli* strain OP50-1 as their standard diet, but for feeding double-stranded RNA to *C. elegans*, to knockdown a gene, we use an *E. coli* strain, HT115, which lacks RNAse III, and therefore does not degrade the double-stranded RNA that is produced in the bacteria.[51] The switch from OP50-1 to HT115 bacteria maintained heritable heat stress resistance and fertility phenotypes but eliminated the subtle increase in lifespan that starved worms display on OP50-1 (Figure S6B). Therefore, we could not test whether DIMT-1 was necessary for the intergenerational lifespan extension in response to parental starvation. *bud-23(tm5768)* mutant worms displayed no increase in lifespan in the parental generation in response to starvation (Figure S6C), suggesting that BUD-23 is required for the extension in lifespan in response to starvation. Therefore, we could not examine whether BUD-23 was necessary for the intergenerational lifespan extension in response to parental starvation. Similarly to the knockdown phenotypes, the *bud-23* genetic mutant, *tm5768*, while generally more stress resistant and less fertile than WT worms, still displayed an increase in heat stress resistance and a reduction in fertility in response to starvation in the parental generation (Figures 5E and 5F), but did not transmit

these phenotypes to their naïve F1 progeny (Figures 5G and 5H). Because *bud-23(tm5768)* mutant worms could still display a significant change in fertility and heat stress response after starvation in the P0 generation (Figures 5E and 5F), these results suggest that both heritable starvation dependent and independent phenotypes can be assessed. We found that WT but not the catalytic dead *bud-23* (Figure 3C) rescued the transmission of the intergenerational heat stress resistance and reduction in fertility (Figures 5I, 5J, S6D, and S6E) suggesting that the intergenerational hormesis phenotype is dependent on the catalytic activity of *bud-23*. Thus, these results suggest that BUD-23 and DIMT-1 are necessary for the transmission of the intergenerational hormesis response to starvation. To determine whether the requirement of the putative 18S rRNA m^7G methylase and the 18S rRNA $m^{6,2}A$ methylase was specific to these enzymes or was more generally a consequence of rRNA modifying enzymes important for ribosome biogenesis, we examined the requirement of other rRNA methyltransferases that are important for ribosomal subunit maturation. We tested *emg-1*, the homolog of EMG1, which is an N1-specific pseudouridine methylase of the 18S rRNA,[52,53] *fib-1*, the 2′-O-ribose methyltransferase that is responsible for methylating more than 100 sites on both the 18S and 28S rRNA,[54] and *nsun-1*, the N5-cytosine methyltransferase of the 28S rRNA.[46,55] We found that knockdown of each of these rRNA methyltransferases decreased fertility and increased heat stress resistance under basal well-fed conditions (Figures 5K and S6F). After knockdown of these enzymes heat stress resistance still increased and fertility still decreased in response to
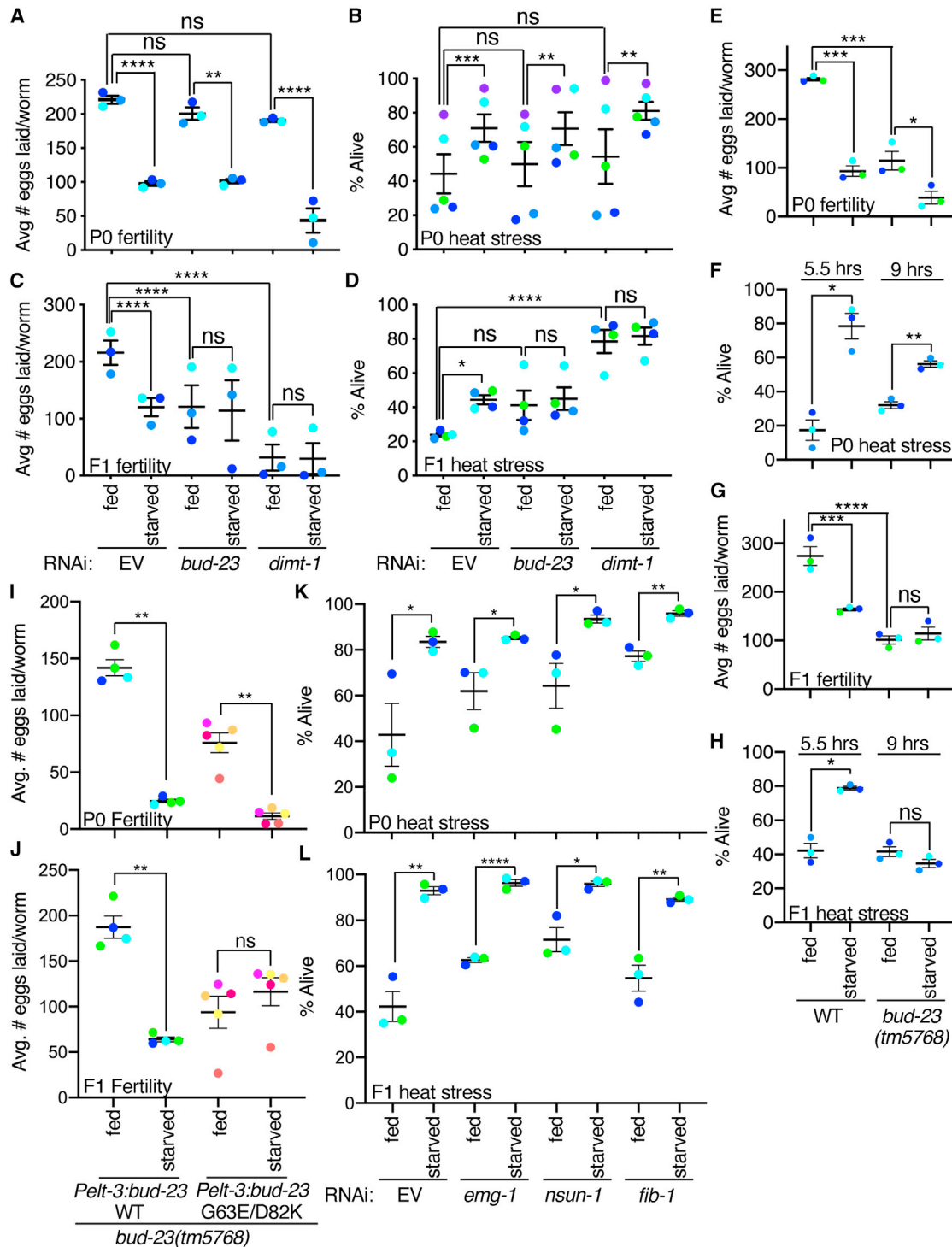
Figure 5. *dimt-1* **and** *bud-23* **are required for intergenerational hormesis**

(A) Starvation causes a reduction in reproduction in worms including when *bud-23* and *dimt-1* are knocked down in the parental P0 generation. Each column represents the mean ± SEM of 3 independent experiments performed in three plates with 10 worms per plate. After starvation, L1 worms were placed on bacteria expressing double-stranded RNA directed against *bud-23, dimt-1*, or an empty vector (EV). Dots are color coded to display matched independent experiments.

(B) Starvation causes an increase in survival in response to 37°C heat stress for 6 h. Each column represents the mean ± SEM of 5 independent experiments performed in three plates with 30 worms per plate.

(legend continued on next page)

starvation (Figures 5K and S6F). However, knockdown of these enzymes had no effect on the transmission of the hormesis phenotypes to the naïve F1 descendants (Figures 5L and S6G) suggesting that they are not required for the transmission of the intergenerational hormesis response to starvation. Thus, the requirement of bud-23 and dimt-1 appears to be specific to these rRNA methyltransferases and is not simply a consequence of altered rRNA methylation. Collectively, these data suggest that in response to starvation, worms transmit elevated N6 dimethylated adenosine 18S rRNA to their naïve progeny, which helps to confer an intergenerational hormesis phenotype.

DISCUSSION

Thus far, correlations have been reported of altered histone modifications, DNA methylation, or small RNA levels in naïve descendants which display transgenerational epigenetic inheritance phenotypes (reviewed in Bošković and Rando,[1] Lim and Brunet,[2] Daxinger and Whitelaw,[3] and Rothi and Greer[56]). Several groups have elegantly demonstrated how histone-modifying enzymes or small RNA machinery are required for transgenerational epigenetic inheritance phenotypes.[1–3,56–59] Work demonstrating the extensive cross-talk between epigenetic molecules makes it inherently difficult to distinguish between molecules that are directly transmitted and initiate epigenetic inheritance signaling cascades versus molecules that are secondary or tertiary consequences of the initiating epigenetic cue.[56] Here, we endeavored to identify critical factors for epigenetic inheritance by unbiased tracking of non-genetic material across generations. We have identified that parents, in response to starvation, transmit increased $m^{6,2}A$ methylated 18S rRNA to their naïve progeny (Figure 2). We further identified that DIMT-1 is the methyltransferase required for N6-dimethylation of adenosines 1735 and 1736 on the 18S rRNA and that BUD-23 is the

putative N7-methyltransferase for guanosine 1531 (Figure 3). We found that these methylations and parental starvation affect the ribosome occupancy of the F1 generation at transcripts involved in longevity regulation, stress response, and reproduction (Figures 4 and S5K–S5Q). Excitingly, we found that BUD-23 and DIMT-1, and not other rRNA methyltransferases, are required for the intergenerational hormesis phenotypes of reduced fertility and increased heat stress in response to parental starvation (Figure 5), suggesting that 18S rRNA $m^{6,2}A$ and m^7G are involved in the inheritance of non-genetic information by altering ribosome heterogeneity rather than through eliciting a general defect in ribosome biogenesis. Together, these data track heritable methylation across a generation and identify methylated rRNA as a necessary carrier of non-genetic information in response to starvation.

Our preferred model is that an altered initial rRNA pool sets up a cascade of events that eventually lead to the observed heritable phenotypes (Figure 6). Some of these subsequent events will directly depend on the initial modified rRNA, but many will depend on downstream consequences of having an altered initial pool in the early developmental stages. C. elegans, like other organisms, is entirely dependent on maternally inherited RNAs during the first cell divisions and does not start producing its own transcripts until later stages.[60] Our hypothesis is that in these early stages, the progeny of starved worms translate a slightly different set of transcripts compared with the progeny of fed worms, partly because of these altered heritably methylated rRNAs. This altered initial translation then leads to many different downstream consequences (altered proteins, small RNAs, lipids, etc.), which cause the nematodes to display different phenotypes after development.

What could be the advantage of transmitting excess premethylated 18S rRNA to progeny of starved parents? Considering both $m^{6,2}A$ on A1850 and A1851 and m^7G on G1639 in mammals

(C) Knockdown of bud-23 and dimt-1 from the P0 decreases the number of progeny per worm in the fed F1 generation; however, this decrease is not further exacerbated by parental starvation as parental starvation decreases fertility in EV controls. Worms were maintained on bacteria expressing double-stranded RNA directed against bud-23, dimt-1, or an empty vector from the L1 stage of the P0 generation and the entirety of the F1 generation. Each column represents the mean ± SEM of 3 independent experiments performed in three plates with 10 worms per plate.

(D) Knockdown of bud-23 and dimt-1 from the P0 increases the 37°C heat stress resistance in the fed F1 generation; however, this increase is not further enhanced by parental starvation as parental starvation increases heat stress resistance after EV control treatment. Each column represents the mean ± SEM of 4 independent experiments performed in 3 plates with 30 worms per plate.

(E) Starvation causes a reduction in fertility in both WT and bud-23(tm5768) mutant worms in the parental P0 generation. Bud-23(tm5768) mutant worms have reduced fertility relative to WT worms. Each column represents the mean ± SEM of 3 independent experiments performed in 3 plates with 10 worms per plate.

(F) Starvation causes an increase in survival in response to 37°C heat stress in both WT and bud-23(tm5768) mutant worms in the P0 generation. Bud-23(tm5768) mutant worms display increased basal heat stress and therefore were maintained at 37°C for 9 h to observe significant fatality relative to WT worms, which were maintained at 37°C for 5.5 h. Each column represents the mean ± SEM of 3 independent experiments performed in 3 plates with 30 worms per plate.

(G) Deletion of bud-23 eliminates the transmission of reduced fertility to naïve F1 progeny whose parents were starved relative to progeny whose parents were fed. Bud-23(tm5768) mutant worms have reduced fertility relative to WT worms; however, this decrease is not further exacerbated by parental starvation as in the WT worms. Each column represents the mean ± SEM of 3 independent experiments performed in 3 plates with 10 worms per plate.

(H) Deletion of bud-23 eliminates the transmission of increased 37°C heat stress survival to naïve progeny whose parents were starved relative to progeny whose parents were fed. Bud-23(tm5768) mutant worms display increased heat stress resistance relative to WT worms; however, this increase is not further enhanced by parental starvation as it is in WT worms. Each column represents the mean ± SEM of 3 independent experiments performed in three plates with 30 worms per plate.

(I and J) Rescue of bud-23(tm5768) with a WT but not a catalytically dead bud-23 rescues the capacity to transmit the starvation-induced reduction in fertility to naïve well-fed progeny. Each column represents the mean ± SEM of 4–5 independent experiments performed in three plates with 30 worms per plate.

(K and L) Knockdown of other rRNA methyltransferases that have been proposed to be important for rRNA processing has no effect on the transmission of increased stress resistance to naïve well-fed children in response to parental starvation. Each column represents the mean ± SEM of 3 independent experiments performed in 3 plates with 30 worms per plate in response to 37°C heat stress for 6–8 h. ns, not significant, * $p < 0.05$, ** $p < 0.01$, *** $p < 0.001$, **** $p < 0.0001$ as assessed by one-way ANOVA with Tukey's or Holm-Sidak's multiple comparisons test.

See also Figure S6.
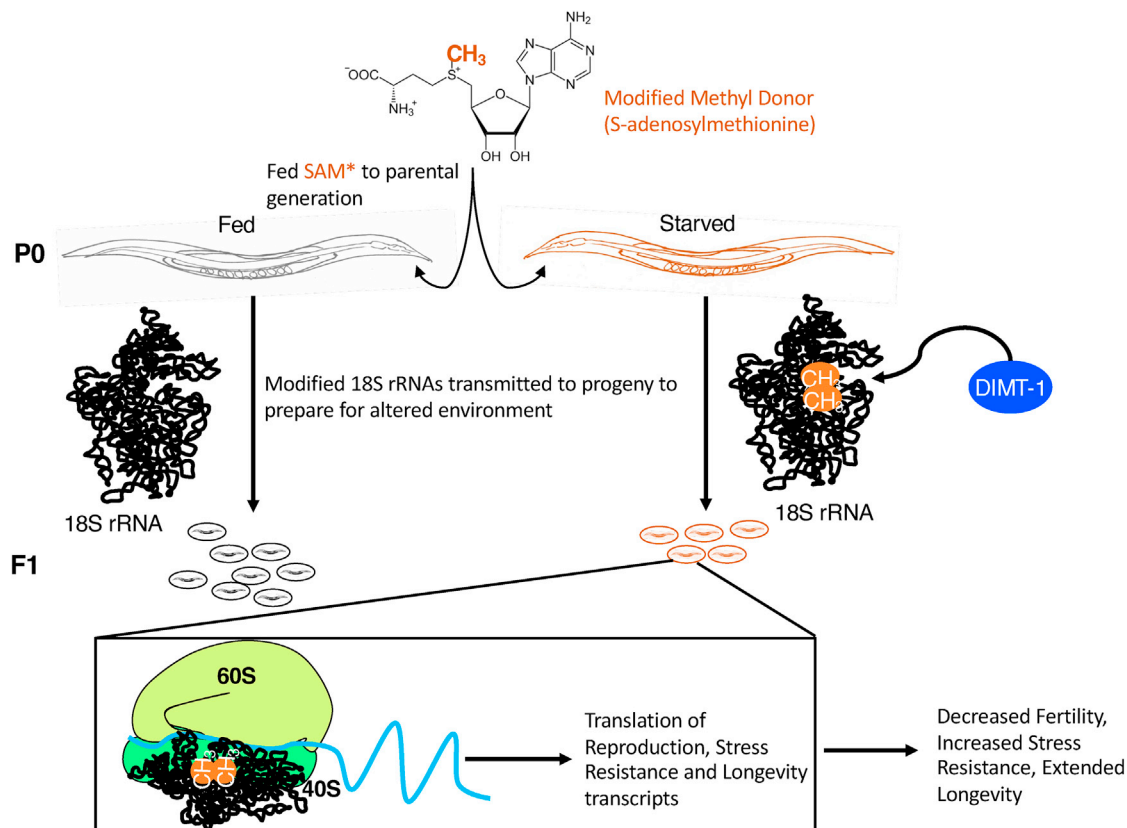
Figure 6. Model of role of 18S rRNA methylation in intergenerational hormesis in response to starvation

By performing metabolic methyl-labeling experiments using a modified methyl donor, we detected a heritable increase in 18S $m^{6,2}A$, which can specify the binding of the ribosome to transcripts important for reproduction, stress resistance, and longevity, which lead to decreased fertility, increased stress resistance, and increased lifespan in naïve descendants.

and the corresponding nucleosides in yeast are located at key areas of the ribosomal subunit, namely: the decoding site, where mRNA is "read" (for A1850 and A1851), and an RNA ridge between the P-site and the E-site tRNA binding sites (for G1639), they are bound to influence and regulate ribosome function.[61] Our examination of *C. elegans* rRNA methylation at these residues suggests that methylation at G1531 is virtually constitutive, while methylation at A1735 and A1736 appears variable. Therefore, it is possible that the starved nematodes are passing along more faithfully processed and methylated rRNAs to their progeny than their fed counterparts. To support this notion, it was recently demonstrated that maternally provided ribosomes are sufficient to allow the worms to proceed to the L1 stage.[62] Although in former works, demethylation and processing of pre-rRNA precursors were shown to be largely coupled, our data suggests a degree of uncoupling where the DIMT-1 depletion was sufficient to reduce $m^{6,2}A$ noticeably to affect the inheritance of non-genetic information but not to a large enough extent to dramatically affect rRNA processing. This finding, in combination with our results demonstrating altered ribosome occupancy on transcripts in response to *dimt-1* knockdown (Figure 4), suggest that the difference in amounts of $m^{6,2}A$ methylated or unmethylated rRNAs in the progeny could cause alterations in ribosome heterogeneity, which would potentially rewire

translation facilitating the translation of stress-specific response and reproduction genes.

The two adjacent N6-dimethylated adenosines on the 18S rRNA are on the top of helix 45, one of the most conserved elements of the ribosome, located right next to the decoding site, which will hold the tRNA as it is linked to the growing polypeptide chain during translation.[34,63] Crystal structure analysis has revealed that methylation of these adenosine residues in *Thermus thermophilus* (*T. thermophilus*) facilitates appropriate packing of the rRNA and that absence of these methylations disrupts the rRNA structure in the A and P sites of the ribosome.[64] These residues are also directly in contact with a ribosomal protein that bridges the large subunit and the small subunit of the ribosome, potentially explaining why these methylation events alter translation efficiency.[61] In bacteria, lack of $m^{6,2}A$ on the small subunit rRNA has been shown to decrease fidelity during elongation[65] and to increase translation from non-AUG codons.[66] *In vitro* translation extracts prepared from Dim1p deficient yeast cells were inefficient.[67] These subtle changes in rRNA structure could therefore explain the altered translation profile we observe in response to starvation and knockdown of *dimt-1* and *bud-23* (Figure 4). It will be interesting, in future experiments, to determine whether there is some unique common property associated with the differentially bound transcripts in response to

parental starvation and knockdown of *dimt-1* and *bud-23* and whether $m^{6,2}A$ on A1735 and A1736 alters the ribosomes capacity to bind to transcripts involved in reproduction, heat stress resistance, and longevity.

We identified several molecules in addition to rRNA that could be heritably methylated (Figure 2A). Since there is only partial overlap between misregulated gene expression and translation in response to *bud-23* and *dimt-1* knockdown and parental starvation (Figure 4), it is probable that other heritable epigenetic information is important for controlling the descendant response to parental starvation. It will be intriguing, in future studies, to examine these methylated molecules, including other types of RNA, proteins, and lipids, and their possible participation in the transfer of information from parents to progeny. It will also be interesting to explore if they respond to environmental stimuli and if they are important for the organism's ability to appropriately respond to extreme environmental cues that their parents or grandparents experienced. Due to the dilution of these metabolic methyl labels after a single generation, it is currently not feasible to examine whether these molecules could be transgenerationally transmitted; however, it will be exciting in subsequent studies to determine what non-genetic information can persist for multiple generations or whether and how a non-genetic cue could be reacquired for a specific number of generations.

Limitations of the study
Although we do not observe a global change in $m^{6,2}A$ on mRNAs when we deplete nematodes of *bud-23* or *dimt-1* (Figure S3A), this does not rule out that some specific mRNAs could be direct targets of DIMT-1 and BUD-23 and be carriers of the epigenetic signal. Because there are over 50 copies of the rRNA in *C. elegans*, it is not presently feasible to directly manipulate the 18S rRNA and test the directness of 18S rRNA $m^{6,2}A$. It will be interesting, in future studies, to directly manipulate the 18S rRNA and to identify whether any rare mRNAs are targets of DIMT-1.

AUTHOR CONTRIBUTIONS

E.L.G. conceived the study and wrote the paper. N.L. and E.L.G. planned the study. N.L. developed and optimized UHPLC-ms/ms methods and metabolic methyl-labeling experiments, produced Figures 2 and S2, generated samples for ribosome and mRNA sequencing, and advised F.G.M., A.F.T., and A.D. M.H.R. produced Figures S3A and S4A and samples for rRNA processing and advised S.D. M.V.G. performed ribosome sequencing and mRNA sequencing experiments and subsequent analysis for Figures 4, S4G, S4H, and S5. C.Z. produced Figures S3D and S4B–S4F. K.B. produced Figures 3D and 3E, generated transgenic rescue worms, and advised A.K.Y. and J.A.H. F.G.M. helped generate Figures 2A and S2. A.K.Y. performed initial UHPLC-ms/ms methods and was advised by K.B. A.F.T. performed initial phenotypic characterization experiments. J.A.H. produced Figure 3C. H.S. and L.R. performed initial metabolic methyl-labeling experiments. A.D. helped optimize phenotypic characterization experiments. S.D. helped produce Figure S4A. D.L.J.L. advised C.Z., V.N.G. advised M.V.G.,

and E.L.G. produced Figures 1, 3A, 3B, 3F, 3G, 3H, 5, 6, S1, S3B, S3C, and S6. All authors discussed the results and commented on the manuscript.

STAR★METHODS

Detailed methods are provided in the online version of this paper and include the following:

- KEY RESOURCES TABLE
- RESOURCE AVAILABILITY
  - Lead contact
  - Materials availability
  - Data and code availability
- EXPERIMENTAL MODEL AND STUDY PARTICIPANT DETAILS
- METHOD DETAILS
  - Metabolic labeling
  - Worm lysis and protein quantification
  - RNA extraction
  - mRNA isolation and rRNA depletion
  - DNA extraction
  - Lipid extraction
  - Scintillation counting
  - UHPLC-ms/ms
  - Recombinant protein
  - Methyltransferase assays
  - Real-time quantitiative polymerase chain reaction (real-time qPCR)
  - Primer extension and rRNA analysis
  - Site-specific cleavage and radioactive-labeling followed by ligation assisted extraction and thin-layer chromatography
  - Lifespan assays
  - Heat stress assays
  - Fertility assays
- QUANTIFICATION AND STATISTICAL ANALYSIS
  - Ribosome profiling
  - Transcriptome and ribosome profiling sequencing and analysis
  - Fluorescent GFP bacteria consumption
  - Transgenic strain creation

SUPPLEMENTAL INFORMATION

Supplemental information can be found online at https://doi.org/10.1016/j.molcel.2023.08.014.

DECLARATION OF INTERESTS

The authors declare no competing interests.

Molecular Cell
Article

CellPress
OPEN ACCESS

REFERENCES

1. Bošković, A., and Rando, O.J. (2018). Transgenerational epigenetic inheritance. Annu. Rev. Genet. *52*, 21–41. https://doi.org/10.1146/annurev-genet-120417-031404.

2. Lim, J.P., and Brunet, A. (2013). Bridging the transgenerational gap with epigenetic memory. Trends Genet. *29*, 176–186. https://doi.org/10.1016/j.tig.2012.12.008.

3. Daxinger, L., and Whitelaw, E. (2012). Understanding transgenerational epigenetic inheritance via the gametes in mammals. Nat. Rev. Genet. *13*, 153–162. https://doi.org/10.1038/nrg3188.

4. Liberman, N., Wang, S.Y., and Greer, E.L. (2019). Transgenerational epigenetic inheritance: from phenomena to molecular mechanisms. Curr. Opin. Neurobiol. *59*, 189–206. https://doi.org/10.1016/j.conb.2019.09.012.

5. Seong, K.H., Li, D., Shimizu, H., Nakamura, R., and Ishii, S. (2011). Inheritance of stress-induced, ATF-2-dependent epigenetic change. Cell *145*, 1049–1061. https://doi.org/10.1016/j.cell.2011.05.029.

6. Klosin, A., Casas, E., Hidalgo-Carcedo, C., Vavouri, T., and Lehner, B. (2017). Transgenerational transmission of environmental information in C. elegans. Science *356*, 320–323. https://doi.org/10.1126/science.aah6412.

7. Schott, D., Yanai, I., and Hunter, C.P. (2014). Natural RNA interference directs a heritable response to the environment. Sci. Rep. *4*, 7387. https://doi.org/10.1038/srep07387.

8. Lang-Mladek, C., Popova, O., Kiok, K., Berlinger, M., Rakic, B., Aufsatz, W., Jonak, C., Hauser, M.T., and Luschnig, C. (2010). Transgenerational inheritance and resetting of stress-induced loss of epigenetic gene silencing in Arabidopsis. Mol. Plant *3*, 594–602. https://doi.org/10.1093/mp/ssq014.

9. Migicovsky, Z., Yao, Y., and Kovalchuk, I. (2014). Transgenerational phenotypic and epigenetic changes in response to heat stress in Arabidopsis thaliana. Plant Signal. Behav. *9*, e27971. https://doi.org/10.4161/psb.27971.

10. Ito, H., Gaubert, H., Bucher, E., Mirouze, M., Vaillant, I., and Paszkowski, J. (2011). An siRNA pathway prevents transgenerational retrotransposition in plants subjected to stress. Nature *472*, 115–119. https://doi.org/10.1038/nature09861.

11. Rechavi, O., i-Ze'evi, L., Anava, S., Goh, W.S.S., Kerk, S.Y., Hannon, G.J., and Hobert, O. (2014). Starvation-induced transgenerational inheritance of small RNAs in C. elegans. Cell *158*, 277–287. https://doi.org/10.1016/j.cell.2014.06.020.

12. Houri-Zeevi, L., Teichman, G., Gigold, H., and Rechavi, O. (2019). Stress resets transgenerational small RNA inheritance. bioRxiv. https://doi.org/10.1101/669051.

13. Houri-Zeevi, L., Korem Kohanim, Y., Antonova, O., and Rechavi, O. (2020). Three rules explain transgenerational small RNA inheritance in C. elegans. Cell *182*, 1186–1197.e12. https://doi.org/10.1016/j.cell.2020.07.022.

14. Demoinet, E., Li, S., and Roy, R. (2017). AMPK blocks starvation-inducible transgenerational defects in Caenorhabditis elegans. Proc. Natl. Acad. Sci. USA *114*, E2689–E2698. https://doi.org/10.1073/pnas.1616171114.

15. Jobson, M.A., Jordan, J.M., Sandrof, M.A., Hibshman, J.D., Lennox, A.L., and Baugh, L.R. (2015). Transgenerational effects of early life starvation on growth, reproduction, and stress resistance in Caenorhabditis elegans. Genetics *201*, 201–212. https://doi.org/10.1534/genetics.115.178699.

16. Webster, A.K., Jordan, J.M., Hibshman, J.D., Chitrakar, R., and Baugh, L.R. (2018). Transgenerational effects of extended Dauer diapause on starvation survival and gene expression plasticity in Caenorhabditis elegans. Genetics *210*, 263–274. https://doi.org/10.1534/genetics.118.301250.

17. Jimenez-Chillaron, J.C., Isganaitis, E., Charalambous, M., Gesta, S., Pentinat-Pelegrin, T., Faucette, R.R., Otis, J.P., Chow, A., Diaz, R., Ferguson-Smith, A., et al. (2009). Intergenerational transmission of glucose intolerance and obesity by in utero undernutrition in mice. Diabetes *58*, 460–468. https://doi.org/10.2337/db08-0490.

18. Lumey, L.H., Stein, A.D., Kahn, H.S., and Romijn, J.A. (2009). Lipid profiles in middle-aged men and women after famine exposure during gestation: the Dutch Hunger Winter Families Study. Am. J. Clin. Nutr. *89*, 1737–1743. https://doi.org/10.3945/ajcn.2008.27038.

19. Painter, R.C., Osmond, C., Gluckman, P., Hanson, M., Phillips, D.I., and Roseboom, T.J. (2008). Transgenerational effects of prenatal exposure to the Dutch famine on neonatal adiposity and health in later life. BJOG *115*, 1243–1249. https://doi.org/10.1111/j.1471-0528.2008.01822.x.

20. Pembrey, M.E., Bygren, L.O., Kaati, G., Edvinsson, S., Northstone, K., Sjostrom, M., and Golding, J.; ALSPAC Study Team (2006). Sex-specific, male-line transgenerational responses in humans. Eur. J. Hum. Genet. *14*, 159–166. https://doi.org/10.1038/sj.ejhg.5201538.

21. Cheng, Q., Trangucci, R., Nelson, K.N., Fu, W., Collender, P.A., Head, J.R., Hoover, C.M., Skaff, N.K., Li, T., Li, X., et al. (2020). Prenatal and early-life exposure to the Great Chinese Famine increased the risk of tuberculosis in adulthood across two generations. Proc. Natl. Acad. Sci. USA *117*, 27549–27555. https://doi.org/10.1073/pnas.2008336117.

22. Li, Y., He, Y., Qi, L., Jaddoe, V.W., Feskens, E.J., Yang, X., Ma, G., and Hu, F.B. (2010). Exposure to the Chinese famine in early life and the risk of hyperglycemia and type 2 diabetes in adulthood. Diabetes *59*, 2400–2406. https://doi.org/10.2337/db10-0385.

23. Champe, P.C., and Harvey, R.A. (1994). Lippincott's Illustrated Reviews: Biochemistry, Second Edition (Lippincott Williams & Wilkins).

24. Mann, M.B., and Smith, H.O. (1977). Specificity of Hpa II and Hae III DNA methylases. Nucleic Acids Res. *4*, 4211–4221. https://doi.org/10.1093/nar/4.12.4211.

25. Boulias, K., Toczydłowska-Socha, D., Hawley, B.R., Liberman, N., Takashima, K., Zaccara, S., Guez, T., Vasseur, J.J., Debart, F., Aravind, L., et al. (2019). Identification of the m(6)Am methyltransferase PCIF1 reveals the location and functions of m(6)Am in the transcriptome. Mol. Cell *75*, 631–643.e8. https://doi.org/10.1016/j.molcel.2019.06.006.

26. Wang, R., Zheng, W., Yu, H., Deng, H., and Luo, M. (2011). Labeling substrates of protein arginine methyltransferase with engineered enzymes and matched S-adenosyl-L-methionine analogues. J. Am. Chem. Soc. *133*, 7648–7651. https://doi.org/10.1021/ja2006719.

27. Islam, K., Zheng, W., Yu, H., Deng, H., and Luo, M. (2011). Expanding cofactor repertoire of protein lysine methyltransferase for substrate labeling. ACS Chem. Biol. *6*, 679–684. https://doi.org/10.1021/cb2000567.

28. Greer, E.L., Maures, T.J., Hauswirth, A.G., Green, E.M., Leeman, D.S., Maro, G.S., Han, S., Banko, M.R., Gozani, O., and Brunet, A. (2010). Members of the H3K4 trimethylation complex regulate lifespan in a germline-dependent manner in C. elegans. Nature *466*, 383–387.

29. Greer, E.L., Beese-Sims, S.E., Brookes, E., Spadafora, R., Zhu, Y., Rothbart, S.B., Aristizábal-Corrales, D., Chen, S., Badeaux, A.I., Jin, Q., et al. (2014). A histone methylation network regulates transgenerational epigenetic memory in C. elegans. Cell Rep. *7*, 113–126. https://doi.org/10.1016/j.celrep.2014.02.044.

30. Liberman, N., O'Brown, Z.K., Earl, A.S., Boulias, K., Gerashchenko, M.V., Wang, S.Y., Fritsche, C., Fady, P.E., Dong, A., Gladyshev, V.N., et al. (2020). N6-adenosine methylation of ribosomal RNA affects lipid oxidation and stress resistance. Sci. Adv. *6*, eaaz4370. https://doi.org/10.1126/sciadv.aaz4370.

31. Parks, L.W., and Schlenk, F. (1958). The stability and hydrolysis of S-adenosylmethionine; isolation of S-ribosylmethionine. J. Biol. Chem. *230*, 295–305.

32. Morana, A., Stiuso, P., Colonna, G., Lamberti, M., Cartenì, M., and De Rosa, M. (2002). Stabilization of S-adenosyl-L-methionine promoted by trehalose. Biochim. Biophys. Acta *1573*, 105–108. https://doi.org/10.1016/s0304-4165(02)00333-1.

33. Blobel, G., and Potter, V.R. (1967). Studies on free and membrane-bound ribosomes in rat liver. I. Distribution as related to total cellular RNA. J. Mol. Biol. *26*, 279–292.

34. Sergiev, P.V., Aleksashin, N.A., Chugunova, A.A., Polikanov, Y.S., and Dontsova, O.A. (2018). Structural and evolutionary insights into ribosomal RNA methylation. Nat. Chem. Biol. *14*, 226–235. https://doi.org/10.1038/nchembio.2569.

35. Suvorov, A.N., van Gemen, B., and van Knippenberg, P.H. (1988). Increased kasugamycin sensitivity in Escherichia coli caused by the presence of an inducible erythromycin resistance (erm) gene of Streptococcus pyogenes. Mol. Gen. Genet. *215*, 152–155. https://doi.org/10.1007/BF00331317.

36. Lafontaine, D., Delcour, J., Glasser, A.L., Desgrès, J., and Vandenhaute, J. (1994). The DIM1 gene responsible for the conserved m6(2)Am6(2)A dimethylation in the 3′-terminal loop of 18 S rRNA is essential in yeast. J. Mol. Biol. *241*, 492–497. https://doi.org/10.1006/jmbi.1994.1525.

37. Shen, H., Stoute, J., and Liu, K.F. (2020). Structural and catalytic roles of the human 18S rRNA methyltransferases DIMT1 in ribosome assembly and translation. J. Biol. Chem. *295*, 12058–12070. https://doi.org/10.1074/jbc.RA120.014236.

38. Zorbas, C., Nicolas, E., Wacheul, L., Huvelle, E., Heurgué-Hamard, V., and Lafontaine, D.L. (2015). The human 18S rRNA base methyltransferases DIMT1L and WBSCR22-TRMT112 but not rRNA modification are required for ribosome biogenesis. Mol. Biol. Cell *26*, 2080–2095. https://doi.org/10.1091/mbc.E15-02-0073.

39. White, J., Li, Z., Sardana, R., Bujnicki, J.M., Marcotte, E.M., and Johnson, A.W. (2008). Bud23 methylates G1575 of 18S rRNA and is required for efficient nuclear export of pre-40S subunits. Mol. Cell. Biol. *28*, 3151–3161. https://doi.org/10.1128/MCB.01674-07.

40. Haag, S., Kretschmer, J., and Bohnsack, M.T. (2015). WBSCR22/Merm1 is required for late nuclear pre-ribosomal RNA processing and mediates N7-methylation of G1639 in human 18S rRNA. RNA *21*, 180–187. https://doi.org/10.1261/rna.047910.114.

41. Lafontaine, D., Vandenhaute, J., and Tollervey, D. (1995). The 18S rRNA dimethylase Dim1p is required for pre-ribosomal RNA processing in yeast. Genes Dev. *9*, 2470–2481. https://doi.org/10.1101/gad.9.20.2470.

42. Zhu, C., Yan, Q., Weng, C., Hou, X., Mao, H., Liu, D., Feng, X., and Guang, S. (2018). Erroneous ribosomal RNAs promote the generation of antisense ribosomal siRNA. Proc. Natl. Acad. Sci. USA *115*, 10082–10087. https://doi.org/10.1073/pnas.1800974115.

43. Liu, N., Parisien, M., Dai, Q., Zheng, G., He, C., and Pan, T. (2013). Probing N6-methyladenosine RNA modification status at single nucleotide resolution in mRNA and long noncoding RNA. RNA *19*, 1848–1856. https://doi.org/10.1261/rna.041178.113.

44. Liu, K., Santos, D.A., Hussmann, J.A., Wang, Y., Sutter, B.M., Weissman, J.S., and Tu, B.P. (2021). Regulation of translation by methylation multiplicity of 18S rRNA. Cell Rep. *34*, 108825. https://doi.org/10.1016/j.celrep.2021.108825.

45. Basu, A., Das, P., Chaudhuri, S., Bevilacqua, E., Andrews, J., Barik, S., Hatzoglou, M., Komar, A.A., and Mazumder, B. (2011). Requirement of rRNA methylation for 80S ribosome assembly on a cohort of cellular internal ribosome entry sites. Mol. Cell. Biol. *31*, 4482–4499. https://doi.org/10.1128/MCB.05804-11.

46. Schosserer, M., Minois, N., Angerer, T.B., Amring, M., Dellago, H., Harreither, E., Calle-Perez, A., Pircher, A., Gerstl, M.P., Pfeifenberger, S., et al. (2015). Methylation of ribosomal RNA by NSUN5 is a conserved mechanism modulating organismal lifespan. Nat. Commun. *6*, 6158. https://doi.org/10.1038/ncomms7158.

47. Ingolia, N.T., Ghaemmaghami, S., Newman, J.R., and Weissman, J.S. (2009). Genome-wide analysis in vivo of translation with nucleotide resolution using ribosome profiling. Science *324*, 218–223. https://doi.org/10.1126/science.1168978.

48. Proshkin, S., Rahmouni, A.R., Mironov, A., and Nudler, E. (2010). Cooperation between translating ribosomes and RNA polymerase in transcription elongation. Science *328*, 504–508. https://doi.org/10.1126/science.1184939.

49. Burmann, B.M., Schweimer, K., Luo, X., Wahl, M.C., Stitt, B.L., Gottesman, M.E., and Rösch, P. (2010). A NusE:NusG complex links transcription and translation. Science *328*, 501–504. https://doi.org/10.1126/science.1184953.

50. Holdorf, A.D., Higgins, D.P., Hart, A.C., Boag, P.R., Pazour, G.J., Walhout, A.J.M., and Walker, A.K. (2020). WormCat: an online tool for annotation and visualization of Caenorhabditis elegans Genome-Scale Data. Genetics *214*, 279–294. https://doi.org/10.1534/genetics.119.302919.

51. Timmons, L., Court, D.L., and Fire, A. (2001). Ingestion of bacterially expressed dsRNAs can produce specific and potent genetic interference in Caenorhabditis elegans. Gene *263*, 103–112. https://doi.org/10.1016/s0378-1119(00)00579-5.

52. Liu, P.C., and Thiele, D.J. (2001). Novel stress-responsive genes EMG1 and NOP14 encode conserved, interacting proteins required for 40S ribosome biogenesis. Mol. Biol. Cell *12*, 3644–3657. https://doi.org/10.1091/mbc.12.11.3644.

53. Wurm, J.P., Meyer, B., Bahr, U., Held, M., Frolow, O., Kötter, P., Engels, J.W., Heckel, A., Karas, M., Entian, K.D., et al. (2010). The ribosome assembly factor Nep1 responsible for Bowen-Conradi syndrome is a pseudouridine-N1-specific methyltransferase. Nucleic Acids Res. *38*, 2387–2398. https://doi.org/10.1093/nar/gkp1189.

54. Tollervey, D., Lehtonen, H., Jansen, R., Kern, H., and Hurt, E.C. (1993). Temperature-sensitive mutations demonstrate roles for yeast fibrillarin in pre-rRNA processing, pre-rRNA methylation, and ribosome assembly. Cell *72*, 443–457. https://doi.org/10.1016/0092-8674(93)90120-f.

55. Sharma, S., Yang, J., Watzinger, P., Kötter, P., and Entian, K.D. (2013). Yeast Nop2 and Rcm1 methylate C2870 and C2278 of the 25S rRNA, respectively. Nucleic Acids Res. *41*, 9062–9076. https://doi.org/10.1093/nar/gkt679.

56. Rothi, M.H., and Greer, E.L. (2023). From correlation to causation: the new frontier of transgenerational epigenetic inheritance. BioEssays *45*, e2200118. https://doi.org/10.1002/bies.202200118.

57. Gaydos, L.J., Wang, W., and Strome, S. (2014). Gene repression. H3K27me and PRC2 transmit a memory of repression across generations and during development. Science *345*, 1515–1518. https://doi.org/10.1126/science.1255023.

58. Kaletsky, R., Moore, R.S., Vrla, G.D., Parsons, L.R., Gitai, Z., and Murphy, C.T. (2020). C. elegans interprets bacterial non-coding RNAs to learn pathogenic avoidance. Nature *586*, 445–451. https://doi.org/10.1038/s41586-020-2699-5.

59. Wang, S.Y., Kim, K., O'Brown, Z.K., Levan, A., Dodson, A.E., Kennedy, S.G., Chernoff, C., and Greer, E.L. (2022). Hypoxia induces transgenerational epigenetic inheritance of small RNAs. Cell Rep. *41*, 111800. https://doi.org/10.1016/j.celrep.2022.111800.

60. Edgar, L.G., Wolf, N., and Wood, W.B. (1994). Early transcription in Caenorhabditis elegans embryos. Development *120*, 443–451. https://doi.org/10.1242/dev.120.2.443.

61. Sharma, S., and Lafontaine, D.L.J. (2015). 'View From A Bridge': a new perspective on eukaryotic rRNA base modification. Trends Biochem. Sci. *40*, 560–575. https://doi.org/10.1016/j.tibs.2015.07.008.

62. Cenik, E.S., Meng, X., Tang, N.H., Hall, R.N., Arribere, J.A., Cenik, C., Jin, Y., and Fire, A. (2019). Maternal ribosomes are sufficient for tissue

diversification during embryonic development in C. elegans. Dev. Cell *48*, 811–826.e6. https://doi.org/10.1016/j.devcel.2019.01.019.

63. Polikanov, Y.S., Melnikov, S.V., Söll, D., and Steitz, T.A. (2015). Structural insights into the role of rRNA modifications in protein synthesis and ribosome assembly. Nat. Struct. Mol. Biol. *22*, 342–344. https://doi.org/10.1038/nsmb.2992.

64. Demirci, H., Murphy, F.t., Belardinelli, R., Kelley, A.C., Ramakrishnan, V., Gregory, S.T., Dahlberg, A.E., and Jogl, G. (2010). Modification of 16S ribosomal RNA by the KsgA methyltransferase restructures the 30S subunit to optimize ribosome function. RNA *16*, 2319–2324. https://doi.org/10.1261/rna.2357210.

65. van Buul, C.P., Visser, W., and van Knippenberg, P.H. (1984). Increased translational fidelity caused by the antibiotic kasugamycin and ribosomal ambiguity in mutants harbouring the ksgA gene. FEBS Lett. *177*, 119–124. https://doi.org/10.1016/0014-5793(84)80994-1.

66. O'Connor, M., Thomas, C.L., Zimmermann, R.A., and Dahlberg, A.E. (1997). Decoding fidelity at the ribosomal A and P sites: influence of mutations in three different regions of the decoding domain in 16S rRNA. Nucleic Acids Res. *25*, 1185–1193. https://doi.org/10.1093/nar/25.6.1185.

67. Lafontaine, D.L., Preiss, T., and Tollervey, D. (1998). Yeast 18S rRNA dimethylase Dim1p: a quality control mechanism in ribosome synthesis? Mol. Cell. Biol. *18*, 2360–2370. https://doi.org/10.1128/MCB.18.4.2360.

68. Liao, S., Chen, X., Xu, T., Jin, Q., Xu, Z., Xu, D., Zhou, X., Zhu, C., Guang, S., and Feng, X. (2021). Antisense ribosomal siRNAs inhibit RNA polymerase I-directed transcription in C. elegans. Nucleic Acids Research *49*, 9194–9210. https://doi.org/10.1093/nar/gkab662.

69. Schneider, C. A., Rasband, W. S., and Eliceiri, K. W. (2012). NIH Image to ImageJ: 25 years of image analysis. Nature Methods *9*, 671–675. https://doi.org/10.1038/nmeth.2089.

70. Martin, M. (2011). Cutadapt removes adapter sequences from high-throughput sequencing reads. EMBnet.journal *17*. https://doi.org/10.14806/ej.17.1.200.

71. Dobin, A., Davis, C.A., Schlesinger, F., Drenkow, J., Zaleski, C., Jha, S., Batut, P., Chaisson, M., and Gingeras, T.R. (2013). STAR: ultrafast universal RNA-seq aligner. Bioinformatics *29*, 15–21. https://doi.org/10.1093/bioinformatics/bts635.

72. Love, M.I., Huber, W., and Anders, S. (2014). Moderated estimation of fold change and dispersion for RNA-seq data with DESeq2. Genome Biol. *15*, 550. https://doi.org/10.1186/s13059-014-0550-8.

73. Subramanian, A., Tamayo, P., Mootha, V.K., Mukherjee, S., Ebert, B.L., Gillette, M.A., Paulovich, A., Pomeroy, S.L., Golub, T.R., Lander, E.S., et al. (2005). Gene set enrichment analysis: a knowledge-based approach for interpreting genome-wide expression profiles. Proc. Natl. Acad. Sci. USA *102*, 15545–15550. https://doi.org/10.1073/pnas.0506580102.

74. Brenner, S. (1974). The genetics of Caenorhabditis elegans. Genetics *77*, 71–94.

75. Boulias, K., and Greer, E.L. (2021). Detection of DNA methylation in genomic DNA by UHPLC-MS/MS. Methods Mol. Biol. *2198*, 79–90. https://doi.org/10.1007/978-1-0716-0876-0_7.

76. Su, D., Chan, C.T., Gu, C., Lim, K.S., Chionh, Y.H., McBee, M.E., Russell, B.S., Babu, I.R., Begley, T.J., and Dedon, P.C. (2014). Quantitative analysis of ribonucleoside modifications in tRNA by HPLC-coupled mass spectrometry. Nat. Protoc. *9*, 828–841. https://doi.org/10.1038/nprot.2014.047.

77. Bar, D.Z., Charar, C., Dorfman, J., Yadid, T., Tafforeau, L., Lafontaine, D.L., and Gruenbaum, Y. (2016). Cell size and fat content of dietary-restricted Caenorhabditis elegans are regulated by ATX-2, an mTOR repressor. Proc. Natl. Acad. Sci. USA *113*, E4620–E4629. https://doi.org/10.1073/pnas.1512156113.

78. Heissenberger, C., Rollins, J.A., Krammer, T.L., Nagelreiter, F., Stocker, I., Wacheul, L., Shpylovyi, A., Tav, K., Snow, S., Grillari, J., et al. (2020). The ribosomal RNA m(5)C methyltransferase NSUN-1 modulates healthspan and oogenesis in Caenorhabditis elegans. eLife *9*. https://doi.org/10.7554/eLife.56205.

79. Greer, E.L., Dowlatshahi, D., Banko, M.R., Villen, J., Hoang, K., Blanchard, D., Gygi, S.P., and Brunet, A. (2007). An AMPK-FOXO pathway mediates longevity induced by a novel method of dietary restriction in C. elegans. Curr. Biol. *17*, 1646–1656.

80. Aeschimann, F., Xiong, J., Arnold, A., Dieterich, C., and Großhans, H. (2015). Transcriptome-wide measurement of ribosomal occupancy by ribosome profiling. Methods *85*, 75–89. https://doi.org/10.1016/j.ymeth.2015.06.013.

81. Gerashchenko, M.V., and Gladyshev, V.N. (2017). Ribonuclease selection for ribosome profiling. Nucleic Acids Res. *45*, e6. https://doi.org/10.1093/nar/gkw822.

82. Mello, C.C., Kramer, J.M., Stinchcomb, D., and Ambros, V. (1991). Efficient gene transfer in C. elegans: extrachromosomal maintenance and integration of transforming sequences. EMBO J. *10*, 3959–3970.

STAR★METHODS

KEY RESOURCES TABLE

REAGENT or RESOURCE	SOURCE	IDENTIFIER
Bacterial and virus strains		
Escherichia coli	New England Biolabs	BL21
Escherichia coli	New England Biolabs	NEB C2925
Chemicals, peptides, and recombinant proteins		
SAM-^{3}H$_3$	PerkinElmer	NET155H001MC
Methionine-^{3}H$_3$	PerkinElmer	NET061X001MC
SAM-D$_3$	Sigma	A7007
Methionine-D$_3$	Cayman	34826
SuperScript® III Reverse Transcriptase	Thermo	18080044
RNAse H	New England Biolabs	M0297
RNAse A/T1	Thermo	EN0551
RNase S7	Roche	50-100-3364
Novex 2X TBE-Urea Sample Buffer	Thermo	LC6876
RNasin	Promega	N2615
Nuclease P1	Wako	145-08221
DNA Degradase Plus	Zymo	E2021
Nucleoside Digestion Mix	New England Biolabs	M069S
rSAP	New England Biolabs	M0371
T4 PNK	New England Biolabs	M0201
[γ-^{32}P]ATP	Perkin Elmer	NEG002A001MC
T4 DNA ligase	New England Biolabs	M0437
TURBO DNase	Ambion	AM2239
SuperScript® III First-Strand Synthesis System	Thermo	18080051
iTaq Universal SYBR® Green Supermix	Bio-Rad	1725121
Critical commercial assays		
Bradford assay	Bio-Rad	5000002
Pierce™ BCA Protein Assay Kit	ThermoFisher	23225
PureLink RNA Mini Kit	Invitrogen	12183018A
Direct-zol RNA Kit	Zymo	R2051
Zymoclean Gel RNA Recovery Kit	Zymo	D4007
Oligo d(T25) Magnetic Beads	New England Biolabs	S1419S
RiboMinus™ Eukaryote Sytem v2	Invitrogen	A15020
TRIzol	Invitrogen	15596026
TRI reagent	Invitrogen	AM9738
Bio-Spin 5 column	Bio-Rad	7326002
Fuji Imaging Plate	Fujifilm	ST-6/HR-6/ST-BD/HR-BD
PEI-cellulose Plate	Merck Millipore	105579
BAS storage phosphor screen	GE Healthcare Life Sciences	29175523
Amicon filter columns	Millipore	UFC5003BK
Novex 15% TBE-Urea gel	Life Technologies	EC6885BOX
Novex 6% TBE-Urea gel	Life Technologies	EC6865BOX
TruSeq Small RNA kit	Illumina	RS-200-0012
1-kb DNA ladder	Invitrogen	10-787-018

Molecular Cell
Article

CellPress
OPEN ACCESS

Continued

REAGENT or RESOURCE	SOURCE	IDENTIFIER
Deposited data		
Raw and analyzed data	This paper	GEO: GSE175363
Unprocessed Images	This paper	https://doi.org/10.17632/wd4tg4mjfp.2
Experimental models: Organisms/strains		
C. elegans: Strain N2 Bristol	Caenorhabditis Genetics Center	N2
C. elegans: Strain *bud-23*	Shouhoung Guang Lab	*tm5768*
Oligonucleotides		
A1735, 1736: GCUGUAGGUGAACCUGCAGCU	This paper	N/A
A1735,1736->G: GCUGUAGGUGGGCCUGCAGCUGG	This paper	N/A
18S F 5′-CGATAACAGGTCTGTGATGCCC-3′	Liao et al.[68]	N/A
18S R 5′-TACCCTATCCCGGACATGGAAG-3′	Liao et al.[68]	N/A
26S F 5′-TAATGTCCTCAACCTATTCTCAA-3′	Liao et al.[68]	N/A
26S R 5′-GCCAGTTCTGCTTACCAA-3′	Liao et al.[68]	N/A
rpl-26 F 5′-CCGATGATGAGGTCGTCGTT-3′	This paper	N/A
rpl-26 R 5′-GCACAGTGGATCCGTTAGCC-3′	This paper	N/A
pan-actin F 5′-TCGGTATGGGACAGAAGGAC-3′		N/A
pan-actin R 5′-CATCCCAGTTGGTGACGATA-3′		N/A
Remaining oligonucleotides in Table S4	Table S4	Table S4
Recombinant DNA		
pSD1::*bud-23*	This paper	N/A
pSD1::*bud-23* G63E/D82K	This paper	N/A
pTG96	Will Mair lab	N/A
Software and algorithms		
Prism 8.4.3	Graphpad	N/A
Chemidoc Image Lab (v4.0)	Bio-Rad	N/A
ImageQuantTL	GE Healthcare Life Sciences	N/A
MassHunter Suite	Agilent	N/A
ImageJ	Schneider et al.[69]	https://imagej.nih.gov/ij/
Cutadapt	Martin[70]	https://github.com/marcelm/cutadapt
STAR	Dobin et al.[71]	https://github.com/alexdobin/STAR
DESeq2	Love et al.[72]	https://bioconductor.org/packages/release/bioc/html/DESeq2.html
GSEA	Subramaniam et al.[73]	https://www.gsea-msigdb.org/gsea/index.jsp
Other		
Bioinformatics pipeline and supplementary code	This paper	https://doi.org/10.5281/zenodo.8231900 and https://github.com/germaximus/Greer_2021

RESOURCE AVAILABILITY

Lead contact
Please contact Eric Lieberman Greer (ericg@wustl.edu) for reagents and resources generated in this study.

Materials availability
Transgenic *C. elegans* lines generated in this study have been deposited to the *Caenorhabditis* Genetics Center.

Data and code availability
- Raw sequencing data can be accessed through the GEO repository. https://www.ncbi.nlm.nih.gov/geo/query/acc.cgi?acc=GSE175363. All original unprocessed images are available in Mendeley Data. All data are publicly available as of the

date of the publications. Accession numbers and DOI are listed in the key resources table.
- All custom code has been deposited to Github and Zenodo. DOI are listed in the key resources table.
- Any additional information required to reanalyze the data reported in this paper is available from the lead contact upon request.

EXPERIMENTAL MODEL AND STUDY PARTICIPANT DETAILS

The N2 Bristol strain of *C. elegans* was used as the wildtype background. Worms were grown on OP50-1 bacteria or *dam⁻dcm⁻* bacteria (NEB C2925) on standard nematode growth medium (NGM) plates[74] in all experiments save for RNAi experiments. Bacteria expressing dsRNA of *bud-23* and *dimt-1* were obtained from the Ahringer and Vidal libraries (a gift from T.K. Blackwell). Bacteria were grown at 37°C and seeded on NGM plates containing ampicillin (100 mg ml⁻¹) and isopropylthiogalactoside (IPTG; 0.4 mM). Each vector was sequenced to verify the presence of the appropriate gene of interest. *bud-23(tm5768)* strain was a gift from Shouhong Guang and was backcrossed 6 times.

METHOD DETAILS

Metabolic labeling
Gravid adult worms were collected in M9 buffer (22 mM KH_2PO_4, 42 mM Na_2HPO_4, 86 mM NaCl, 1 mM $MgSO_4$), washed several times in M9 buffer followed by bleaching (10 N NaOH, NaHOCl, H20 at a 1:1:11.5 ratio) for egg extraction. Eggs were washed thoroughly several times with either M9 buffer or sterile water and plated on the desired food source. When worms reached L4 stage of development (48 hours at 20 ºC), their food source was replaced with concentrated heat killed bacteria and the desired metabolic label. Metabolic labeling was performed by adding either SAM-$^3H_3$ or Methionine-$^3H_3$ (PerkinElmer) at 100-165 μCi or 62.5 mM SAM-D_3 (CDN isotopes) or 250 mM Methionine-D3 (Sigma) to the concentrated bacteria. Unmodified SAM and Methionine were used as negative controls to ensure incorporation occurred during the experiment. It has been shown that SAM is relatively unstable[31,32] and therefore it is most likely that any tritium detected in the progeny would have been incorporated into heritably methylated material in the parents and transmitted to the progeny rather than taken up by the progeny themselves or transmitted in the form of SAM-$^3H_3$ to be used by the progeny themselves. However, this is still a possibility and that is why subsequent genetic experiments demonstrating the requirement of *bud-23* and *dimt-1* help to further solidify the findings. Worms were allowed to continue development until day 1 of egg laying. Worms were removed from plates with M9 buffer and eggs were removed from the plate by using a cell scraper and resuspending in M9 buffer. Worms and eggs were washed several times with M9 buffer. Eggs and any remaining worms were bleached twice followed by several washes in water. Worms were washed twice with 70% Ethanol followed by several washes in water. Worm and Egg samples were flash frozen until processing. For starvation experiments, bleached eggs were plated on NGM plates without food where they hatched and arrested at L1 for 7 days (starved). In parallel a portion of the eggs were plated on NGM with food (fed). Following 7 days the fed population of worms were bleached to extract eggs that were plated on food while the L1 arrested worms were transferred to plates with food 3-4 hours later (initial experiments showed that this allowed both populations to reach the L4 stage when labeling occurs at the same time). Metabolic labeling and collection of the samples occurred as detailed above. Each sample was normalized to the total amount of specific material (DNA, RNA, proteins, lipids) to allow for comparisons between independent measurements. Phenotypic assays following starvation paradigm are detailed below.

Worm lysis and protein quantification
Worm or egg pellets were resuspended in a homemade lysis buffer (20 mM $NaPO_4$, 150 mM NaCl, 1% NP-40, 0.5% DOC, 0.5% SDS, 2 mM EDTA) supplemented with a protease inhibitor cocktail (Roche) and 1 mM DTT, followed by 6-8 freeze thaw cycles in liquid nitrogen and an incubation at 95 °C for 10 minutes. Lysates were cleared by centrifugation at 20,000 g for 10 min at 4 °C. Protein quantification was performed by Bradford (Bio-Rad) or BCA (ThermoFischer) assay.

RNA extraction
RNA from worm and egg samples was extracted either with PureLink RNA Mini Kit (Invitrogen) or Direct-zol RNA kit (Zymo). The worm and egg pellets were resuspended in lysis buffer (either homemade supplemented lysis buffer or the kit lysis buffer) or 1 ml of Trizol, followed by 6-8 freeze thaw cycles in liquid nitrogen. RNA was then extracted according to the manufacturer's protocol. As part of the PureLink kit, samples were homogenized with the homogenizer column (Invitrogen). RNA quantification was performed on either a DeNovix DS-11+ spectrophotometer or a Qubit 3 fluorometer (Invitrogen). To isolate 26S, 18S, and 5.8S/5S rRNAs, total RNA was electrophoresed on agarose gels to separate rRNAs which were excised and purified using either Zymoclean Gel RNA Recovery Kit (Zymo) or ethanol precipitation.

mRNA isolation and rRNA depletion
Total RNA was extracted by addition of 1 ml TRIzol (Invitrogen) to 100 μl of packed worm pellet. Six freeze-thaw cycles were performed in liquid nitrogen. RNA extraction was performed according to the manufacturer's protocol (Invitrogen, TRIzol). To isolate mRNA, 75 μg of RNA was incubated at 65°C for 2 minutes to disrupt secondary structures and placed on ice. 200ul of Oligo

Molecular Cell
Article

CellPress
OPEN ACCESS

d(T$_{25}$) Magnetic Beads (5 mg/ml, New England Biolabs) were washed with 100 μl of 1X Binding Buffer (0.01 M Tris-HCL, pH 7.5; 0.5 M LiCl; 1 mM EDTA) and resuspended with 100 μl of 2X Binding Buffer (0.02 M Tris-HCL, pH 7.5; 1 M LiCl; 2 mM EDTA). RNA was added to the magnetic bead suspension and mixed by pipetting. RNA-beads mix was rotated for 30 minutes at room temperature and then placed in a magnetic rack to remove supernatant. Beads were washed with 200 μl Washing Buffer B (0.01 M Tris-HCL, pH 7.5; 0.15 M LiCl; 1 mM EDTA) twice. 50 μl of Elution Buffer (0.01 M Tris-HCL, pH 7.5) was added to the beads and mixed by pipetting. Samples were incubated at 70°C for 5 mins with shaking at 800 RPM and then placed into a magnetic rack to collect beads. Eluent (RNA) was collected to proceed with the next step. To deplete ribosomal RNA from the mRNA isolate, samples were processed using the RiboMinus™ Eukaryote Sytem v2 (Invitrogen) as described in manufacturer's protocol. Samples were then processed for UHPLC-ms/ms analysis.

DNA extraction
Worms and eggs were resuspended in the supplemented homemade lysis buffer, followed by 6-8 freeze thaw cycles in liquid nitrogen. DNA was then extracted using PureLink Genomic DNA Mini Kit (Invitrogen) according to the manufacturer's protocol. DNA quantification was performed on either a DeNovix DS-11+ spectrophotometer or a Qubit 3 fluorometer (Invitrogen).

Lipid extraction
Worm or egg samples were first lysed according to the protocol detailed above and equal volumes of sample were taken for lipid extraction using a Lipid Extraction kit (BioVision, K216) according to the manufacturer's protocol.

Scintillation counting
Tritium signal was detected by direct addition of the tested sample (RNA, DNA, lipids, lysate) to Econo-Safe (RPI) followed by scintillation counting on a scintillation counter.

UHPLC-ms/ms
DNA samples ranging from 500 ng-2 μg were digested to free nucleosides using 5-15 U of DNA Degradase Plus (Zymo Research) in 25 μl reactions incubated for 2 hrs at 37 °C. For quantification, pure 2'deoxyadenosine (dA) and N6-methyl-2'-deoxyadenosine (6mdA) nucleosides were used as calibration standards. Quantification was performed as in Boulias and Greer,[75] briefly digested samples or pure nucleoside standards were diluted to 100 μl with ddH2O and filtered through 0.22 μm Millex syringe filters and 5 μl of the filtered solution was injected for UHPLC-ms/ms analysis, and analyzed using the Agilent 1290 UHPLC system with a C18 reversed-phase column (2.1 × 50 mm, 1.8 m). Mobile phase A consisted of water with 0.1% (v/v) formic acid and mobile phase B consisted of methanol with 0.1% (v/v) formic acid. Mass spectrometry detection was performed using an Agilent 6470 triple quadrupole mass spectrometer in positive electrospray ionization mode and data were quantified in dynamic multiple reaction monitoring (dMRM) mode, by monitoring the mass transitions 252.1 →136.0 for dA and 266.1→150.0 for 6mdA. The ratio of 6mdA/A was quantified using calibration curves from serial dilutions of pure 6mdA or dA standards. As a negative control in each UHPLC-ms/ms experiment, we included a "mock" digestion reaction, consisting of DNA Degradase Plus and digestion buffer in water, without any added DNA.

To quantify the concentrations of m^{6}A, m^{6,2}A, m^{7}G and m^{5}C in *C. elegans* RNA samples, we used pure nucleosides of adenosine (A), cytidine (C), guanosine (G), N6-methyladenosine (m^{6}A), N6-dimethyladenosine (m^{6,2}A), C5-methylcytidine (m^{5}C), and N7-methylguanosine (m^{7}G) as calibration standards. For digestion to nucleosides, 250 ng – 1 μg of RNA samples were digested with Nucleoside Digestion mix (NEB, M069S) for 2 hr at 37°C. Digested RNA samples or pure nucleoside standards were diluted to 100 μl with ddH20 and filtered through 0.22 μm Millex Syringe Filters. 5 μl of the filtered solution was injected for LC-MS/MS analysis, and analyzed using the Agilent 1290 UHPLC system with a Hypersil Gold C18 reversed-phase column (2.1 x 150 mm, 3 μm) as per Su et al.[76] with modifications listed below. Mobile phase A consisted of water with 0.1% (v/v) formic acid and mobile phase B consisted of acetonitrile with 0.1% (v/v) formic acid. Mass spectrometry detection was performed using an Agilent 6470 triple quadrupole mass spectrometer in positive electrospray ionization mode and data were quantified in dynamic multiple reaction monitoring (dMRM) mode, by monitoring the mass transitions 268 → 136 for Adenosine (A), 282 → 150 for N6-methyladenosine (m^{6}A), 285 → 153 for deuterated N6-methyladenosine (d3-m^{6}A), 244 → 112 for Cytidine (C), 261 → 129 for deuterated C5-methylcytidine (d3-m^{5}C), 284 → 152 for Guanosine (G), 282 → 136 for 2'-O-methyladenosine (Am), 285 → 136 for deuterated 2'-O-methyladenosine (d3-Am), 258 → 112 for 2'-O-methylcytidine (Cm), 261 → 112 for deuterated 2'-O-methylcytidine (d3-Cm), 298 → 152 for 2'-O-methylguanosine (Gm), 301 → 152 for deuterated 2'-O-methylguanosine (d3-Gm), 296 → 164 for N6'-N6-dimethyladenosine (m62A), 302 → 170 for deuterated N6'-N6-dimethyladenosine (d3-m62A), 298 → 166 for N7-methylguanosine (m7G), 301 → 169 for deuterated N7-methylguanosine (d3-m7G), 285 → 153 for deuterated N1-methyladenosine (d3-m^{1}A). The ratio of methylated A (%m^{6}A or % m^{6,2}A) or G (%m^{7}G) in RNA samples was quantified using calibration curves from serial dilutions of the pure ribonucleoside standards.

Recombinant protein
The coding sequence of *dimt-1* was cloned as an in-frame fusion to the GST tagged vector pGEX-4T1. The catalytic site was mutated through site-directed mutagenesis. The recombinant proteins were expressed in *E. coli* BL21. Overnight induction of protein

Molecular Cell
Article

expression was carried out with 1 mM IPTG at 18°C. Bacteria were harvested at 4000 rpm, 4°C and 10 mL protein purification lysis buffer (50 mM pH 7.5 Tris-HCl, 0.25 M NaCl, 0.1% Triton-X, 1 mM PMSF, 1 mM DTT, and protease inhibitors). After freezing the pellet at -80°C for 1 hour, the lysate was sonicated with a Bioruptor for 5 minutes on high level with 30 seconds on and 30 seconds off. Proteins were purified with glutathione Sepharose 4B beads. Proteins and beads were washed 3 times with protein purification lysis buffer before incubating the beads with elution buffer (12 mg/ml Glutathione in protein purification lysis buffer, pH 8.0) for 30 minutes. Eluates were dialyzed overnight at 4°C with dialysis buffer (50 mM pH 8.0 Tris-HCl, 1mM EDTA, 1mM DTT, and 20% glycerol). Bradford assays and SDS-page gel electrophoresis followed by coomassie staining was performed to determine integrity and quantity of purified proteins.

Methyltransferase assays

In vitro methylation reactions assaying methyltransferase activity of *dam* or HpaII (NEB) on DNA were performed in the buffer supplied with the commercial recombinant enzyme (New England Biolabs (NEB) dam Methyltransferase Reaction Buffer or CutSmart Buffer) per the NEB protocol. Methyltransferase activity was assessed on 0.5-2 µg of pL4440 plasmid DNA extracted from dam⁻dcm⁻ bacteria. *In vitro* reactions were performed with 80 µM or 160 µM SAM-D_3 or a mixture of SAM and SAM-D_3 as indicated. Reactions were purified using a PCR purification kit (Invitrogen) followed by digestion with DNA degradase plus (Zymo) for UHPLC-MS/MS analysis. For radioactive *in vitro* assays, 0.4 µM or 3.2 µM of SAM-$^3H_3$ were used and the reaction was cleaned with either a PCR purification kit or Bio-Spin P30 columns (Bio-rad). The reactions were incubated for 2 hrs at 37 °C, followed by enzyme deactivation for 20 minutes at 65 °C. *In vitro* reactions with GST-DIMT-1 were performed as in Shen et al.,[37] briefly 30 µl reactions containing 2 µg of 18S rRNA or oligos were incubated with 12 µgs of DIMT-1 WT or E79A mutant, 1mM d_3-SAM, 50 mM Tris pH 7.5, 5mM MgCl$_2$, and 1 mM DTT at 16°C overnight. Then reactions were incubated for 20 minutes at 65 °C, followed by clean up and buffer exchange with Bio-Spin P30 columns (Bio-rad). RNA was digested to nucleosides with 20 units of S1 Nuclease (ThermoScientific) at 37°C for 2 hours followed by treatment with Fast Alkaline Phosphatase (ThermoScientific) for 1 hour at 37 °C. Samples were diluted 2X with milliQ water and 5 µl were used for UHPLC-MS/MS analysis. Synthesized 18S rRNA oligos of the following sequences: A1735, 1736: GCUGUA GGUGAACCUGCAGCUGG and A1735,1736->G: GCUGUAGGUGGGCCUGCAGCUGG were obtained from IDT.

Real-time quantitiative polymerase chain reaction (real-time qPCR)

Total RNA was extracted by addition of 1 ml TRIzol (Invitrogen) to 100 µl of packed worm pellet. Six freeze-thaw cycles were performed in liquid nitrogen. RNA extraction was performed according to the manufacturer's protocol (Invitrogen, TRIzol). Total RNA was treated with TURBO DNase (Ambion) as described in the manufacturer's protocol to remove contaminating DNA in the sample. cDNA synthesis was performed using SuperScript® III First-Strand Synthesis System as described in the manufacturer's protocol. PCR was performed using iTaq Universal SYBR® Green Supermix (Applied Biosystems) and primers targeting 18S rRNA, 26S rRNA and *rpl-26*. Primers sequences 18S F 5'-CGATAACAGGTCTGTGATGCCC-3', 18S R 5'-TACCCTATCCCGGACATGGAAG-3', 26S F 5'-TAATGTCCTCAACCTATTCTCAA-3', *rpl-26* F 5'-CCGATGATGAGGTCGTCGTT-3', *rpl-26* R 5'-GCACAGTGGATCCGTTAGCC-3' *pan-actin* F 5'-TCGGTATGGGACAGAAGGAC-3', *pan-actin* R 5'-CATCCCAGTTGGTGACGATA-3'.

Primer extension and rRNA analysis

5 µg total RNA extracted using the TRI reagent (Invitrogen) was resolved on a denaturing agarose gel during 18h30 at 65V, stained with ethidium bromide and processed for northern blotting with probe LD2648 (5'-CACTCAACTGACCGTGAAGCCAGTCG-3') or LD2649 (5'-GGACAAGATCAGTATGCCGAGACGCG-3')[77] as in Heissenberger et al.[78] Primer extension was performed with primer LD4728 (5'-GACCGTGAAGCCAGTCGAGCATC-3') on 5 µg total RNA as in Zorbas et al.[38] The northern blot and primer extension assays were exposed to Fuji imaging plates (Fujifilm) and quantification was performed on a phosphorimager (FLA-7000; Fujifilm) using the MultiGauge software (Fujifilm, v 3.1). The signals corresponding to the mature rRNAs were quantified using the chemidoc Image Lab software (v 4.0).

Site-specific cleavage and radioactive-labeling followed by ligation assisted extraction and thin-layer chromatography

Site-specific cleavage and radioactive-labeling followed by ligation assisted extraction and thin-layer chromatography (SCARLET) assays were performed as in Liu et al.[43] Briefly, in the first step 18S rRNA was subjected to RNAse H site-specific cleavage directed by 2'-O-methyl RNA-DNA chimeras with the following sequences; *C. elegans* 18S rRNA G1531 chimeric oligo: 5'- mGmGmCmAmU mUmCCTCGmUmUmUmAmAmGmG-3', *C. elegans* 18S rRNA A1735 chimeric oligo: 5'- mGmCmAmGmGmUmUCACCmUmAmC mAmGmCmU-3', *C. elegans* 18S rRNA A1736 chimeric oligo: 5'- mUmGmCmAmGmGmUTCACmCmUmAmCmAmGmC-3', *H. sapiens* 18S rRNA G1639 chimeric oligo: 5'- mGmGmAmAmUmUmCCTCGmUmUmCmAmUmGmG-3', *H. sapiens* 18S rRNA A1850 chimeric oligo: 5'- mGmCmAmGmGmUmUCACCmUmAmCmGmGmAmA-3'. 200 ng of gel purified 18S rRNA was mixed with 5 pmoles chimeric oligo in 30 mM Tris-HCL, pH=7.5 in a total volume of 5 µl. The resulting mixture was heated for 3 min at 95°C followed by cooling to RT for 3 min. RNAse H (5 Units, NEB), rSAP (1 Unit, NEB) and RNasin (20 units, Promega) were added in a total volume of 10 µl in 1X T4 PNK buffer (NEB) and the mixture was incubated for 1 hr at 44°C, followed by heat inactivation for 5 min at 75°C. Radioactive end-labeling was performed with the addition of T4 PNK (20 Units, NEB) and 2 µl [γ-^{32}P]ATP (6000Ci/ mmol) at 37°C for 1 hr in a total volume of 15 µl in 1X T4 PNK buffer, followed by heat inactivation for 5 min at 75°C. The free

$[\gamma$-^{32}P]ATP was removed by the use of Bio-Spin 6 column (Biorad) according to the manufacturer's instructions. The radioactive labeled 18S fragments were subjected to splint ligation by the addition of 5 pmoles splint oligo and 5 pmoles of 116-mer ssDNA oligo of the following sequences; *C. elegans* 18S rRNA G1531 splint oligo: 5'-AGCTGATGACTCACACTTACTAGGCATTCCTATTAACTCA CAGGACCGGCGATGGCTG-3', *C. elegans* 18S rRNA A1735 splint oligo: 5'-CGATGATCCAGCTGCAGGTTCTATTAACTCACAG GACCGGCGATGGCTG -3', *C. elegans* 18S rRNA A1736 splint oligo: 5'- CGATGATCCAGCTGCAGGTCTATTAACTCACAGGAC CGGCGATGGCTG-3', *H. sapiens* 18S rRNA G1639 splint oligo: 5'- AGCTTATGACCCGCACTTACTGGGAATTCCTATTAACTCAC AGGACCGGCGATGGCTG-3', *H. sapiens* 18S rRNA A1850 splint oligo: 5'- TAATGATCCTTCCGCAGGTTCTATTAACTCACAGGA CCGGCGATGGCTG-3', 116-mer ssDNA oligo: 5'- GGAGAGACAACTTAAAGAGACTTAAAAGATTAATTTAAAATTTATCAAAAAGA GTATTGACTTAAAGTCTAACCTATAGGATACTTACAGCCATCGCCGGTCCTGTGAGTTAATAG-3'. The resulting mixture was heated for 3 min at 75°C followed by cooling to RT for 3 min. Ligation was performed in a total volume of 20 μl by the addition of 1 μl T4 DNA Ligase (400 Units, NEB) in 1X T4 DNA Ligase buffer (NEB) and the mixture was incubated for 3 hr at 37°C. RNA was degraded by the addition of 1 μl RNAseA/T1 mix (Thermo) for 1 hr at 37°C and the ligation reaction was stopped by the addition of 2 μl 500 mM EDTA and 20 μl Novex 2X TBE-Urea Sample buffer (Thermo). The radioactive ligation mixtures were subjected to TBE-urea gel electrophoresis followed by staining with SYBR gold. The band that corresponded to the radiolabeled splint ligated 117/118 bp fragment was excised and was eluted for 3 hr at 37°C in 300 μl gel extraction buffer (300 mM NaOAc pH5.5, 1 mM EDTA, 0.25%v/v SDS), followed by ethanol precipitation. The purified fragment was resuspended in DEPC-treated water and was digested with Nuclease P1 (2 Units, Wako USA) in 10 mM ammonium acetate pH=5.2, 2 mM ZnCl$_2$ for 2 hr at 60°C in a total volume of 20 μl. 2.5 μl of the digested nucleotide mixture was analyzed by TLC on a glass-backed PEI-cellulose plate (Merck Millipore) in a buffer containing isopropanol/HCl/ water (70:15:15). Signal acquisition and quantification of the radiolabeled adenosine and N6-methyladenosine, N6-dimethylated adenosine, Guanosine and N7-methylguanosine was carried out using a BAS storage phosphor screen (GE Healthcare Life Sciences) at 200 μm resolution using the ImageQuantTL software (GE Healthcare Life Sciences).

Lifespan assays
Worm lifespan assays were performed at 20°C, without 5-fluoro-2'-deoxyuridine (FUDR), as described previously[79] unless noted otherwise. For each lifespan assay, ~90 worms per condition were used in three plates to begin the experiment (30 worms per plate). Worms that underwent matricide, exhibited a ruptured vulva, or crawled off the plates were censored. Statistical analysis of lifespan were performed on Kaplan-Meier survival curves in Prism 8.4.3 by log rank (Mantel-Cox) tests. The values from the Kaplan-Meier curves are included in Table S1.

Heat stress assays
Synchronized L4 worms were placed at 37°C for the time indicated and then grown at 20°C for the remainder of the assay. Each experiment included at least 30 worms per plate with three plates per condition. Survival was assessed every 24 hrs after initial heat stress.

25 °C heat stress assays were performed as in Klosin et al.[6] and Schott et al.[7] Briefly, embryos were extracted from gravid adults as described above and plated on NGM plates with food incubated at 20°C or 25 °C. Plates with eggs were incubated either at 20°C or 25 °C. Worm populations that reached the L4 stage (worms at 25°C reached L4 sooner than worms at 20°C) were metabolically labeled and either returned to 20°C or shifted from 25°C to 20°C.

Fertility assays
From day 3 to day 8 post-hatching, 10 worms were placed on NGM plates with dam⁻dcm⁻ bacteria in triplicate (30 worms total per condition). Worms were grown at 20°C. After 24 hrs, the adult worms were removed from each plate and placed on new plate. The numbers of eggs and hatched worms on the plate were counted. Statistical analyses of fertility were performed using t-tests using mean and standard error values.

QUANTIFICATION AND STATISTICAL ANALYSIS

All statistics for lifespan, heat stress, and fertility assays were performed using Prism. The details of the number of replicates and sample sizes are included in each figure legend.

Ribosome profiling
Ribosome profiling was performed according to published protocol[80] with modifications according to published protocols.[81] Flash frozen worm pellets were lysed and homogenized in lysis buffer (20 mM Tris-HCl pH 7.5, 50 mM KCl, 50 mM NaCl, 5 mM MgCl$_2$, 100 μg/ml Cycloheximide, 1 mM DTT, EDTA-free protease inhibitors cocktails (Roche), 1% Triton X100) using pellet pestles for 1.7ml tubes. 10% of each lysate was immediately taken to isolate total RNA by adding 300 μl of Trizol-LS (Invitrogen) and proceeding with Direct-Zol miniprep kit (Zymo). CaCl$_2$ was added to a final concentration of 5 mM to the rest of the lysate. Lysates were treated with 600 U of RNase S7 (Roche) for 1 hour at room temperature. RNA digestion was quenched by supplementing 10 μl of 0.5 M EGTA. Treated lysates were run on sucrose gradients (10-50%) and the monosome peak was collected and concentrated on 100kDa Amicon filter columns (Millipore). RNA from the monosome fraction was extracted using TRIzol LS and a Direct-zol kit (Zymo). The RNA

was loaded on a Novex 15% TBE-Urea gel (Life Technologies) and a range of fragments between 25 and 32 bps were excised and eluted from the gel. The library was prepared using the TruSeq Small RNA kit (Illumina) according to published protocol.[80] The PCR product was then loaded on a Novex 6% TBE-Urea gel (Life Technologies) and a band around 160-170 bp was excised from the gel. The DNA was eluted from the gel and sent for quality assurance and sequencing at the Biopolymers facility at Harvard University. RNA for mRNA sequencing was extracted using Direct-zol and sent for polyA selection, library preparation and sequencing at Novogene Inc.

Transcriptome and ribosome profiling sequencing and analysis

Transcriptomes and ribosome profiling libraries were sequenced on the Illumina NovaSeq 6000 and NextSeq 500 platforms. mRNA libraries were sequenced in a paired-end mode with each read being 150 nucleotides long. Ribosome profiling libraries were sequenced in a single-end mode with 51 nucleotides read length before adapter trimming. Adapters were removed with Cutadapt software,[70] short reads alignment and counting performed with STAR aligner.[71] Differential gene expression was evaluated with the DESeq2 package in the R programming environment.[72] Gene set enrichment analysis was done with GSEA stand-alone software (Broad Institute, [73]) using a collection of *C. elegans* gene lists derived from the gene2go annotation data at the NCBI. They are analogous to the GO-based series of human-only collections available from MSigDB: a source gene list collection used in the original implementation of GSEA software by Broad Institute.

Fluorescent GFP bacteria consumption

Starvation assays were set up as described above. Worms that reached the L4 stage were transferred to plates spotted with OP50-GFP bacteria to feed for 2 hrs. 30 worms were then moved to plates without food for 5 minutes. 10 worms were transferred to 2% agar slides with a drop of 50 mM NaN3 as a paralytic. GFP detection was performed on a Zeiss Discovery V8 fluorescent microscope. GFP fluorescence was quantified using ImageJ.

Transgenic strain creation

Expression vectors for creating transgenic strains were based on pSD1 plasmid vector (a gift from W. Mair and S. Dutta) that contains the ubiquitous *eft-3* promoter and *unc-54* 3′ untranslated region. *Bud-23* and the *bud-23* G63E/D82K catalytic mutant were amplified from the pGEX-4T1 constructs, followed by restriction-free cloning into the pSD1. Germline transformation experiments were performed as described.[82] For the *bud-23* rescue experiments, injection mixes contained pSD1::*bud-23* or pSD1::*bud-23* G63E/D82K plasmids at 50 ng/μl, pTG96 (20 ng/μl; *Psur-5::gfp*) as a cotransformation marker, and 1-kb DNA ladder (80 ng/μl; Invitrogen) as carrier DNA.